Study IId

Assessment of Air Quality based on Past and Ongoing Monitoring Data in FY12

for the

Assessment of Land-based Sources of Air Quality Contaminants in the Binational Border Region of Southwestern New Mexico, Northwestern Chihuahua and West Texas

Prepared for the Department of Health
Office of Border Health
1170 N. Solano Dr.
Las Cruces, NM 88001

Submitted by

Principal Investigators

Dave DuBois
Erin Ward

Additional Contributors:

Ilias Kavouras, UAMS
Marie-Cecile Chalbot, UAMS
Max Bleiweiss, NMSU
Manoj Shukla, NMSU
Michael Baca, NMED
Juan Pedro Margez, UACJ

New Mexico State University
Las Cruces, NM 88003

June 30, 2012

ACKNOWLEDGEMENTS

This project is being carried out by New Mexico State University in association with the University of Texas El Paso, Autonomous University of Juarez (Chihuahua), the Desert Research Institute, and the University of Arkansas for Medical Sciences.

This work is being funded under a MOA 13828 with the New Mexico Department of Health, Office of Border Health.

Mr. Paul Dulin provided overall project management.

Contents

1. Introduction

This report summarizes the work done to characterize past and present air quality in the study region. It is divided into five major sections: effects of wildfires on ozone, analysis of PM_{10} and $PM_{2.5}$ in the region, the use of remote sensing in determining air quality, the Palomas-Columbus special PM10 study, and finally a microscopic analysis of aerosol samples.

2. Effects of Regional Wildfires on Ozone Levels, Asthma, and COPD Hospitalizations

The US Environmental Protection Agency (EPA) enacted the primary and secondary national ambient air quality standards for atmospheric ozone (O_3) to protect the human health and environmental ecosystems, respectively. The latest revision in 2008 requires that the 3-year average of the fourth highest daily 8-hr running average concentration should not exceed 0.075 ppmv (from 0.084 ppmv enacted in 1997) (US EPA 1997, 2008). Non-attainment areas (violation of the NAAQS for O_3) include metropolitan and surrounding communities across the country and rural regions in the vicinity of oil and gas exploration activities (Schnell et al., 2009; EPA, 2011).

The formation of O_3 during transport from upwind natural and anthropogenic sources of NOx and VOCs is an important contributor to elevated ozone concentrations and exceedances of the O_3 NAAQS standards at many urban and continental background sites. Emissions of O_3 precursors from wildfires frequently exceeded emissions from light-duty gasoline vehicle emissions affecting O_3 concentrations up to 60 ppb in receptor sites within 10 to 100 km of the fire (Junquera et al., 2005). Intercontinental transport of fires emissions in Siberia, Asia and Alaska increased the O_3 levels in mainland US and over Europe triggering violations of the O_3 NAAQS (Jaffe et al., 2004; Pfister et al., 2006). An increasing trend in the O_3 concentrations at Class I protected areas in the US was observed (NPS 2006). This trend was partially attributed to increased temperatures but recent studies indicated that changes in the spatial distribution and intensity of anthropogenic emissions and increased wildfires emissions may also be responsible (Jaffe and Ray, 2007).

Fire frequency and intensity are extremely sensitive to changes in land use practices and El Niño-Southern Oscillation with increases in the number and sizes of wildfires. Over the past two decades, burned areas in the U.S. and Canada exceeded 22,000 km^2/year and 60,000 km^2/year, respectively, which is about three times higher than the 1920-1980 period (Schoennagel et al., 2004; Stocks et al., 2002; Gillet et al., 2004). The increase in the quantity and magnitude of fires is even more pronounced for forests in the western US (Westerling et al., 2006). Longer summers, which are driven by increasing temperatures, increase the fire ignition risk by 10-to-

30% and are expected to increase burned areas by as much as 120% by the end of the century. These projections are direr for higher elevations where wildfire occurrences are more frequent and earlier snowmelts are extending the annual window for wildfires (Flannigan et al., 2004; Running, 2006; Westerling et al., 2006).

The Paso del Norte region encompasses the metropolitan El Paso area in Texas, the greater Las Cruces area in southwestern New Mexico and the Juarez metropolitan area in Mexico (Fig.1). Ambient O_3 concentrations in El Paso, Texas and portions of Doña Ana County are below the NAAQS values despite the significant reductions in NOx emissions from local sources, increased scavenging of O_3 precursors by precipitation and infrequent formation of shallow boundary layers (Sather and Cavender, 2012). The objectives of this effort were to determine the long-term spatial and temporal trends of O_3 levels in the binational border region of southwestern New Mexico, El Paso and Ciudad Juarez area and, assess the effect of wildfires on them. It is part of larger effort to characterize sources and trends of air pollution in the region and their potential impacts on human health.

2.1. Data Acquisition and Reduction

Hourly O_3 measurements at 23 sites in southwestern NM, southeastern AZ, and the Paso del Norte region during the 1993-2010 period were retrieved from the US EPA Air Quality System (AQS) and Clean Air Status and Trends Network (CASTNET) using federal reference methods. The locations of ozone monitoring sites since 1993 are illustrated in Figure 2.1-1.

Figure 2.1-1. Map showing the boundaries of the study domain (a) and the locations of the O3 monitoring sites in Arizona and western New Mexico (b) and, El Paso, Las Cruces and Ciudad Juarez (c)

Table 2.1-1 presents the characteristics and monitoring periods for each site. Chiricahua site in Arizona (AIRS 04-003-8001; ch in Figure 2.1-1) is located within the Chiricahua National Monument Class I protected area and it is operated by the US National Park Service. Ten sites are operated by the New Mexico Environment Department (NMED), three of them within Las Cruces (nm3, nm4 and nm5 in Figure 2.1-1), four of them in the Sunland Park border region (nm5, nm7, nm8, nm9 and nm10 in Figure 2.1-1) and the remaining three in rural communities (nm1, nm2 and nm6 in Figs. 2.1-1b and 2.1-1c. Two sites (35-013-0019 and 35-013-1012) discontinued in 2002 and 2004, and three sites (35-029-0003, 35-017-1003 and 35-013-0023) started after 2004. There are 7 sites within El Paso metropolitan area and 4 sites at Ciudad Juarez in Mexico. These sites were operated by the Texas Commission on Environmental Quality (TCEQ). Two of the sites (48-141-0028 (ep5) and 80-006-0001(cj3)) moved to another locations within a few hundred of meters in 1999 (48-141-0055 (ep6)) and 1998 (80-006-0007(cj4)), respectively. These sites were treated separately to minimize the effect of differences on O_3 measurements caused by the micro-environmental conditions of the monitoring site (e.g. distance to the nearest street and orientation, prevalence of wind conditions).

Table 2.1-1 Site characteristics and O_3 monitoring periods

Site code[a]	Site name	AIRS code[a]	Latitude (°), longitude (°) and elevation (m)	Monitoring period
ch	Chiricahua Nat.M.	04-003-8001	32.117; -109.467; 1570	1989-2010
nm1	Chino Cu-smelter	35-017-1003	32.692; -108.124; 1823	2004-2010
nm2	Deming	35-029-0003	32.256; -107.723; 1313	2006-2010
nm3	6ZL	35-013-0019	32.425; -106.674; 1189	1995-2002
nm4	6ZQ	35-013-0023	32.318; -106.768; 1219	2004-2010
nm5	Las Cruces-Holiday Inn	35-013-1012	32.281; -106.767; 1188	1993-2004
nm6	6ZK	35-013-0020	32.041; -106.409; 1250	1996-2010
nm7	6ZN	35-013-0022	31.788; -106.683; 1280	1996-2010
nm8	6ZM	35-013-0021	31.796; -106.584; 1219	1996-2010
nm9	Sunland Park	35-013-0017	31.796; -106.558; n.a.	1993-2011
nm10	La Union-St. Lukes	35-013-0008	31.931; -106.631; 1204	1993-2010
ep1	El Paso UTEP	48-141-0037	31.768; -106.501; 1158	1993-2010
ep2	Campbell and Franklin	48-141-0027	31.763; -106.487; 1140	1993-2000
ep3	El Paso Chamizal	48-141-0044	31.766; -106.455; 1158	1994-2010
ep4	Skyline Park	48-141-0058	31.894; -106.426; 1201	2000-2010
ep5	Ascarate Park NW	48-141-0028	31.754; -106.404; 1126	1993-1999
ep6	Ascarate Park SE	48-141-0055	31.747; -106.403; 1122	1999-2010
ep7	Lee Trevino and Ivanhoe	48-141-0029	31.786; -106.324; 1239	1998-2010
ep8	Socorro	48-141-0057	31.662; -106.303; 1109	1999-2010
cj1	SITE 20/30	80-006-0006	31.736; -106.46; n.a.	1997-2010
cj2	El Cid and Parque	80-006-0004	31.69; -106.46; n.a.	1994-2010
cj3	Industria & Fernandez NE	80-006-0001	31.719; -106.396; n.a.	1994-1998
cj4	Industria & Fernandez SE	80-006-0007	31.712; -106.395; n.a.	1999-2010

The monthly 8-hour maximum O_3 concentration was computed for months with more than 75 percent valid estimates of daily 8-hr maximum O_3 concentrations for days with more than 18 valid estimates of the 8-hr running averages. The use of the monthly 8-hr maximum O_3 concentration as an indicator was corroborated by previous evidence that wildfires contribute episodically to exceedances of O_3 NAAQS at receptor sites several days or weeks following the fire (Junquera et al., 2004; Jaffe et al., 2004; Pfister et al., 2006; Kavouras et al., 2012). The 25 year time series of 8-hr ozone design (the 4-th highest 8-hr running averages) values and the non-overlapping block five year averages of the percentage of 8-hr averages above the 2008 NAAQS value for the summer months were previously used by Sather and Cavender (2012) to evaluate the compliance with the NAAQS value and to smooth the effects of local meteorology and short-term changes in local emissions. The average monthly O_3 concentration was used as an indicator to detect the effect of temperature variation and aloft O_3 in IMPROVE sites along the Pacific Northwest (Jaffe and Ray, 2007).

The fire detection data and temperature abnormalities for the northern America were retrieved from the USDA Forest Service MODIS Active Fire Mapping Program with a spatial resolution of 1 km. The detections were observed by both Terra and Aqua instruments of MODIS and processed by the USDA Forest Service Remote Sensing Applications Center, NASA-Goddard Space Flight Center and the University of Maryland. The date and locations of fire detections were extracted and the number of fires within 100, 100-250, 250-500, 500-1000, 1000-2000 and 2000-3000 miles buffer zones from each site was estimated for each calendar month during the 2001-2010 period.

Hospitalization counts and rates for residents in the New Mexico counties are retrieved from the State of New Mexico's, Department of Health, Indicator Based Information System for Public Health (NM-IBIS) Hospital Impatient Discharge Data (HIDD). The hospital discharge data are used to track disease rates, spatiotemporal trends, demographic characteristics and the effects of behavioral and environmental risk factors. The Hospital Inpatient Discharge Data include primary/secondary diagnosis for COPD, asthma and stroke (but not for heart failure) when a patient was admitted to a hospital overnight and leaves that hospital. The primary diagnosis is the condition to be responsible for the admission of the patient to the hospital. The secondary diagnosis includes the condition that coexist at the time of inpatient admission which affect the treatment received and/or length of stay. Data from federal facilities (military and veteran's affairs hospitals) and Indian health service facilities are not included.

2.2. Statistical Analysis

Ordinary least squares (OLS) regression analysis of deseasonalized monthly 8-hr maximum O_3 concentrations was used to determine the trends of O_3 without the seasonal component (Jaffe and Ray, 2007). De-seasonalized concentrations were calculated using the "Census I" method integrated in SPSS. The Pearson correlation coefficient (R) was applied to determine whether O_3 concentrations decrease or increase simultaneously. The absolute (ΔC) and the relative ($\%\Delta C/Ref$) differences of 8-hr maximum monthly concentrations between two sites were computed to evaluate concentration gradients in the region. The O_3 monitor at Chiricahua National Monument (EPA AIRS 04-003-8001) was the reference site because of its continental background and upwind location with respect to the other sites in the study domain. The relative concentration differences were computed as the percentage of the absolute concentration difference to the reference site concentration. Positive values indicate that O_3 concentrations at the site were higher than those measured at Chiricahua NM. The coefficient of divergence (COD) was used to assess the spatial uniformity of measurements with respect to the concentration levels (Equation 1).

$$COD = \sqrt{\frac{1}{p} \cdot \sum_{i=1}^{p} \left(\frac{C_{ij} - C_{ik}}{C_{ij} + C_{ik}} \right)^2}$$ (Equation 1)

where p is the total number of paired measurements, and Cij and Cik are the measured concentrations at the reference and comparison sites on the i-th month, respectively (Pinto et al., 2004; Lianou et al., 2007). COD values vary from 0 to 1, with COD values close to unity being suggestive of strong spatial variation.

The contribution of fires on O_3 concentrations was evaluated by multivariate regression analysis. Initially, each calendar month was binned into one of four categories based on the frequency of fires as compared to the total number of fires over the 2001-2010 period in each buffer zone. The 25-th, 50-th and 75-th percentiles were applied as cutpoints for months with: (i) low fire frequency(=1) (less than the 25-th percentile); (ii) moderate fire frequency(=2) (between 25-th and 50-th percentiles); (iii) high fire frequency(=3) (between 50-th and 75-th percentiles) and; (iv) extreme fire frequency(=4) (higher than the 75-th percentiles). The dependent variable was the 8-hr maximum O_3 concentration for i-month and the independent variables were the categories of fire frequencies (Xij: X=1,2,3 or 4) for i-th month in j-th buffer zone (Equation 2).

$$[O_3]_i = a + \sum_{j=1}^{6} (b_j \cdot X_{ij})$$ (Equation 2)

The intercept, a , was attributed to ozone concentrations from non-fire local and regional sources.

2.3. Annual Trends and Spatiotemporal Correlations

Table 2.3-1 shows the annual trends of deseasonalized 8-hr maximum O_3 concentrations for each site (ppbv/yr), the COD and the median (and standard deviation (σ)) of absolute (ΔC) and relative (%ΔC/Ref) concentration differences.

Table 2.3-1 Annual trends of deseasonalized O_3 concentrations, absolute (ΔC) and relative (%ΔC/Ref) concentration differences and COD ratio.

Site code	Annual trend (ppbv/yr)	R^2	2010 8-hr max	ΔC Median (σ)	%ΔC/Ref Median (σ)	COD
ch	0.12[b]	0.13	74			
nm1	0.26	0.08	79	-2 (10)	-5 (13)	0.10
nm2	-1.85[a]	0.16	65	-1 (11)	-2 (16)	0.10
nm3	-0.27	0.01		-1 (4)	-2 (8)	0.04
nm4	-0.22	0.01	68	-2 (7)	-4 (11)	0.06
nm5	-0.07	0.05		1 (10)	1 (16)	0.08

Site code	Annual trend (ppbv/yr)	R^2	2010 8-hr max	ΔC Median (σ)	%ΔC/Ref Median (σ)	COD
nm6	-0.37[a]	0.09	70	1 (8)	1 (13)	0.06
nm7	-0.69[a]	0.25	67	-6 (4)	-10 (8)	0.07
nm8	-0.69[a]	0.18	81	-9 (9)	-15 (11)	0.13
nm9	-0.77[a]	0.26	85	-4 (4)	-8 (7)	0.06
nm10	-0.46[a]	0.17	70	-9 (6)	-17 (10)	0.11
ep1	0.13	0.07	88	-12 (17)	-21 (25)	0.21
ep2	-2.77[a]	0.24		-1 (19)	-2 (26)	0.17
ep3	-0.50[a]	0.07	76	-4 (9)	-6 (16)	0.08
ep4	-0.15	0.01	77	-5 (14)	-9 (21)	0.14
ep5	2.38[a]	0.37		-4 (14)	-8 (22)	0.14
ep6	0.07	0.03	77	-7 (12)	-13 (21)	0.11
ep7	-0.51	0.08	71	-7 (10)	-11 (17)	0.10
ep8	-0.15[b]	0.15	77	-2 (9)	-3 (16)	0.07
cj1	-1.21[a]	0.18	79	5 (23)	7 (32)	0.21
cj2	-1.22[a]	0.21	60	-6 (16)	-10 (25)	0.16
cj3	-0.65	0.01		-11 (14)	-17 (25)	0.17
cj4	-1.00[a]	0.13	88	-1 (14)	-2 (24)	0.11

[a] significant at $p < 0.001$; [b] significant at $p<0.01$

The observed trends were statistically significant at α=99.9% in twelve sites and at a=99% in two sites. Most of the sites (18 of 23) showed trends from -0.07 to -1.85 ppbv/yr in Deming, NM (nm3 in Figure 2.1-1). The three sites within the Las Cruces urban area (nm3, nm4 and nm5 in Fig.1c), demonstrated a statistically insignificant trend from -0.07 to -0.27 ppbv/yr. However, for sites located on the southeast part of the Doña Ana county (nm6 – nm10 in Figure 2.1-1), the decreasing trends were higher (from -0.37 to -0.77 ppbv/yr) and statistically significant at α=99%. All sites at Ciudad Juarez in Mexico (cj1-cj4 in Figure 2.1-1) experienced a decrease of more than 1 ppbv/yr on the monthly 8-hr maximum O_3 concentrations. In El Paso, annual trends from -0.15 to -0.51 ppbv/yr were estimated in four site (two of them were statistically significant). Positive trends (but statistically insignificant) of 0.07 and 0.13 ppbv/yr were computed for ep1 and ep6 site (Figure 2.1-1). Two sites exhibited statistically significant trends of -2.77 (ep2) and 2.38 (ep5) ppbv/yr; however these sites were decommissioned in 2000 and 1999, respectively. The annual trends of their replacement sites (ep3 and ep6, respectively) were -0.50 (a=99.9%) and +0.07 ppbv/yr. For the Chiricahua site, a statistically significant positive trend (0.12 ppbv/yr) was observed. This was in agreement with the observed increase of the monthly mean O_3 concentrations in other Class I protected areas in western United States (Jaffe and Ray, 2007).

The observed positive trends on both monthly mean (Jaffe and Ray, 2007) and 8-hr maximum concentration (this study) in continental background sites contradicted the decreasing trends of O_3 concentrations in urban areas (Sather and Cavender, 2012) and underlined the complexity of reducing O_3 concentrations over large geographic areas. Adjustments for meteorological

conditions showed very little effect on O_3 trends in urban and continental background locations in the western US (EPA, 2008). Other factors including increasing global background O_3 concentrations due to increased emissions from developing countries in Asia and increased emissions from more frequent and intense wildfires may be important determinants of this variability. In addition, spatiotemporal changes of NOx and VOCs emissions (e.g. due to expansion of small size cities and rural communities) may also be an important determinant of the observed positive trends in background sites but have very little effect on existing urban populated areas.

Figure 2.3-1 shows the distribution of Pearson correlation coefficients of deseasonalized monthly 8-hr maximum O_3 concentrations for each site. The correlation coefficients were above 0.7 among the sites within the extended Las Cruces – El Paso- Ciudad Juarez sites (nm4-nm10, ep1-ep8, cj1-cj4 in Figure 2.3-1) (except for ep2, ep5 and cj3 which were terminated before 2000) indicating a temporal uniformity of elevated O_3 levels in the populated regions. On the contrary, moderate R values (median of 0.7 and lower) were computed for the Chiricahua site (ch) and the two sites located in rural communities in west New Mexico (nm1 and nm2 in Figure 2.1-1) demonstrating the different temporal trends in urban and non-urban sites. Meanwhile, the values of the COD (from 0.06 to 0.21), absolute (less than 12 ppbv) and relative (less than 21%) concentrations differences for each site using the Chiricahua site as reference indicated the absence of a spatial gradient of the monthly 8-hr maximum O_3 concentrations. The highest absolute and relative concentration differences were estimated for the site in the University of Texas, El Paso which is located downwind of the El Paso-Ciudad Juarez downtown complex. The site-to-site variation of O_3 concentrations (described by the standard deviations of ΔC and %ΔC/Ref) suggested common characteristics for El Paso-Ciudad Juarez sites. Overall, these findings indicated important qualitative differences on the trends and timings of elevated O_3 concentrations; however, the absolute O_3 concentrations did not vary a lot.

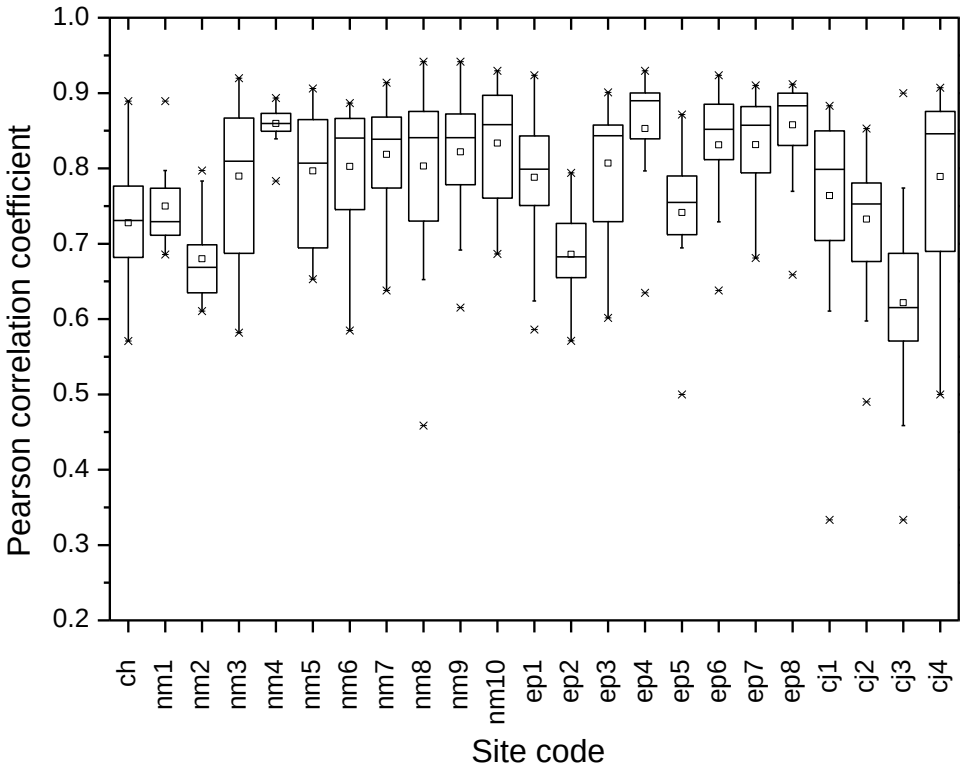

Figure 2.3-1. Distribution of Pearson correlation coefficients for monthly 8-hr maximum O_3 concentrations for each site. For each box plot, the middle line represents the median value, the solid square represents the mean value, the box includes the 25th and 75th percentiles and whiskers represent the 5th and 95th percentiles.

2.4. Effects of wildfires on ozone levels

This section attempts to apportion the contributions of wildfires on elevated O_3 concentrations. Figure 2.4-1 illustrates the mean of monthly 8-hr maximum O_3 concentrations for months with low, moderate, high and extreme fire frequencies in each buffer zone for Chiricahua (ch in Figure 2.4-1), sites in southwest New Mexico (nm1 and nm2 in Figure 2.1-1), Las Cruces sites (nm3, nm4 and nm5 in Figure 2.1-1), Sunland Park sites (nm6 through nm10 in Figure 2.1-1), El Paso sites (ep1 through ep8 in Figure 2.1-1) and Ciudad Juarez sites (cj1 to cj4 in Figure 2.1-1). For fire detections within 100 miles, the O_3 concentration for months with low fire frequency was higher (from 2 to 8 ppbv) than the O_3 concentrations measured for months with moderate and high fire frequencies for all locations (except Chiricahua). For sites in El Paso and Ciudad Juarez, the O_3 concentrations measured during months of extreme fire frequencies within 100 miles remained lower than those measured for months with low fire frequency. The same trend (decreasing O_3 concentrations for months with higher fire frequencies) was observed sites in Sunland Park, El Paso and Ciudad Juarez for fire detections in the 100-250 buffer zones, too.

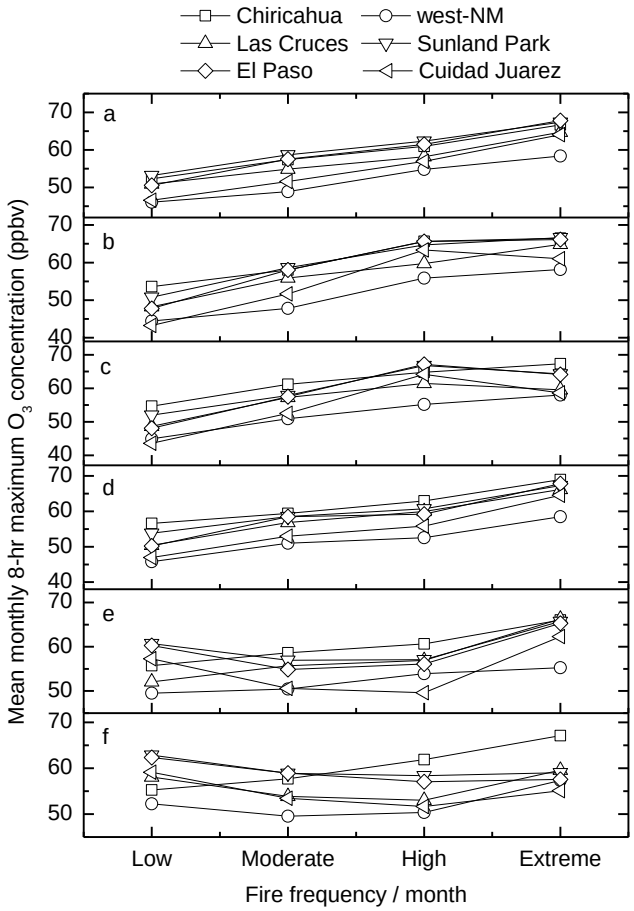

Figure 2.4-1. Monthly 8-hr maximum O_3 concentration for months with low (<25th percentile), moderate (25-50th percentile), high (50-75th percentile) and extreme (>75th percentile) fire frequencies for each buffer

These trends indicated that emissions of O_3 precursors from fires were mixed with local anthropogenic emissions in the urban populated areas triggering the destruction of O_3 (Junquera et al., 2004). For Chiricahua site, O_3 concentrations increased as much as 12 ppbv for months with extreme fire frequencies within 100 and 100-250 miles, indicating that fire emissions increase O_3 concentrations in receptor sites within 100 miles of the fire. For fires incidents at more than 250 miles, the O_3 concentrations for all locations increased as a function of fire frequencies. The trends appeared to be similar for all sites with an increase of 12-17 ppbv of O_3 concentration for months high extreme fire frequency as compared to months with low fire frequencies. These similarities indicated that O_3 was formed aloft from fire-related VOCs and NOx emissions during transport and it was mixed with ground-level O_3.

Table 2.4-1. Buffer and net (absolute and percentage) contributions of wildfires on the monthly 8-hr maximum O_3 concentrations

Site code	Buffer contribution (ppbv)[a]						Net (ppbv)	% of 8-hr max O_3
	>100 miles	*100 – 250 miles*	*250 – 500 miles*	*500 – 1000 miles*	*1000 – 2000 miles*	*2000 – 3000 miles*		
ch	**3**	-1	**1**	0	**2**	**2**	**7**	12%
nm1	-1	-1	0	-1	**5**	**2**	**4**	9%
nm2	-2	-3	1	-2	**5**	**4**	**3**	6%
nm3	0	-1	4	4	0	0	7	11%
nm4	-5	-1	**4**	1	**3**	**4**	**6**	12%
nm5	0	0	**3**	-1	**7**	-2	**7**	14%
nm6	**-4**	**-4**	**6**	-1	**6**	**4**	**7**	12%
nm7	**-5**	**-6**	**8**	-1	**5**	**4**	**5**	8%
nm8	**-5**	**-5**	**7**	-2	**4**	**4**	**3**	5%
nm9	**-3**	**-4**	**5**	-1	**4**	**3**	**4**	7%
nm10	**-2**	-3	**6**	-1	**3**	**3**	**6**	11%
ep1	**-6**	**-7**	**11**	1	2	**5**	**6**	10%
ep2	**-6**	**-6**	**11**	-1	5	**4**	**7**	13%
ep3	**-4**	**-5**	**9**	-2	**4**	**3**	**5**	9%
ep4	**-5**	**-6**	**11**	1	1	**5**	**7**	13%
ep5	**-5**	**-5**	**8**	1	3	**4**	**6**	11%
ep6	**-4**	**-6**	**8**	**5**	0	**4**	**7**	13%
ep7	**-5**	-4	**9**	-3	**6**	**7**	**10**	22%
ep8	-3	-4	**5**	-1	3	**4**	**4**	8%
cj1	**-5**	**-8**	**12**	0	3	**4**	**6**	10%

[a] Significant estimates (at *p-value* < 0.15) are in bold

The contributions of fires in each buffer zone were computed for each site by multivariate linear regression (Equation 2). Table 2.4-2 shows the contribution of fires in each buffer zone, the absolute net and percentage contribution of monthly 8-hr maximum O_3 concentrations. Differences between sites in populated communities and background sites have been also detected. For all the sites (with the exception of Chiricahua), 8 hr-maximum O_3 concentrations decreased by as much as 8 ppbv for fires within 250 miles of the sites (estimates were statistically significant at p-value < 0.15). A net positive contribution of 2 ppbv was estimated for Chiricahua for fires within 250 miles. A radical change was observed for fires in the 250-500 miles buffer zone, with positive contribution from 1 up to 12 ppbv (statistically significant at p-value < 0.15) in all sites. Statistically insignificant contributions were computed for fires in the 500-1000 miles buffer zone. However, for fires incidents at more than 1000 miles away from the sites, statistically significant contributions (from 4 to 13 ppbv) were calculated. Overall,

wildfires contributed from 3 to 10 ppbv on the highest monthly 8-hr O_3 concentration, which occasionally may trigger violation of the NAAQS for O_3. The estimated contributions represented from 9 to 22 percent of measured monthly 8-hr maximum concentrations, which were comparable to those computed by Pfister et al., (2006).

Fires near the receptor site modified the irradiated VOCs-to-NOx mixture which triggered in the formation or destruction of O_3 depending on the local conditions. Table 2.4-3 shows the National Emission Inventory (NEI) 2008 annual emissions of NOx and VOCs for each county in the study domain. NOx emissions in Cochise County, AZ (Chiricahua site) were higher than those measured in New Mexico Counties and about 20% lower than those computed for El Paso. For most of the counties (except Cochise, AZ and Luna, NM), the estimated VOCs emissions were comparable to NOx emissions. While, the chemical composition of VOCs modifies the ozone formation potential, the county-based emissions demonstrated VOCs-limited conditions in Cochise County, and NOx-limited conditions in Doña Ana in NM and El Paso in Texas (NOx limited). Thus, emissions of VOCs from wildfires near the sites would trigger O_3 formation in Chiricahua but have very little or negative effect in the urban populated sites. Fires further away contributed through the mixing of aloft O_3 formed during transport with ground-level air.

Table 2.4-2. NEI 2008 annual emissions of NO_x, VOCs and speciated gas-phase volatile hazardous air pollutants (in tons)

County	NOx	VOCx	Volatile HAPs
Cochise, AZ	14,384	6,768	2,558,915
Graham, AZ	975	1,751	606,282
Doña Ana, NM	8,501	7,359	2,455,451
Grant, NM	1,582	1,369	500,657
Hidalgo, NM	1,869	575	200,436
Luna, NM	3,266	1,711	573,248
Otero, NM	2,473	2,583	925,487
Sierra, NM	1,292	1,613	690,676
El Paso, TX	17,872	16,310	4,481,442

The spatial variations of normalized fires detection (number of fires detections in the cell /total number of fires detection in the buffer zone) for 0.25° x 0.25° cells in the 250-500 miles (a) and 1000-3000 miles (b) buffer zones for sites in Las Cruces-El Paso-Ciudad Juarez region are depicted in Figure 2.4-2. Three areas in central Arizona, central Texas and south Sonora/north Sinaloa in Mexico experienced the highest frequencies of fire detections in the 250-500 miles buffer zone. For the combined 1000-3000 buffer zones, extreme fire frequencies were observed along the Colorado Rockies in Idaho and British Columbia, in southeast US (Alabama, Georgia and Florida), central Mexico, Cuba and Jamaica. As part of the assessment of causes of haze in

Class I protected areas in the western regional air partnership domain, the analysis of backward trajectories residence times for Class I sites in south New Mexico and southwest Texas showed that air masses in May-June period originated from northern and western Mexico, while for summer months, air masses came from the Gulf of Mexico and Cuba (COHA, 2006).

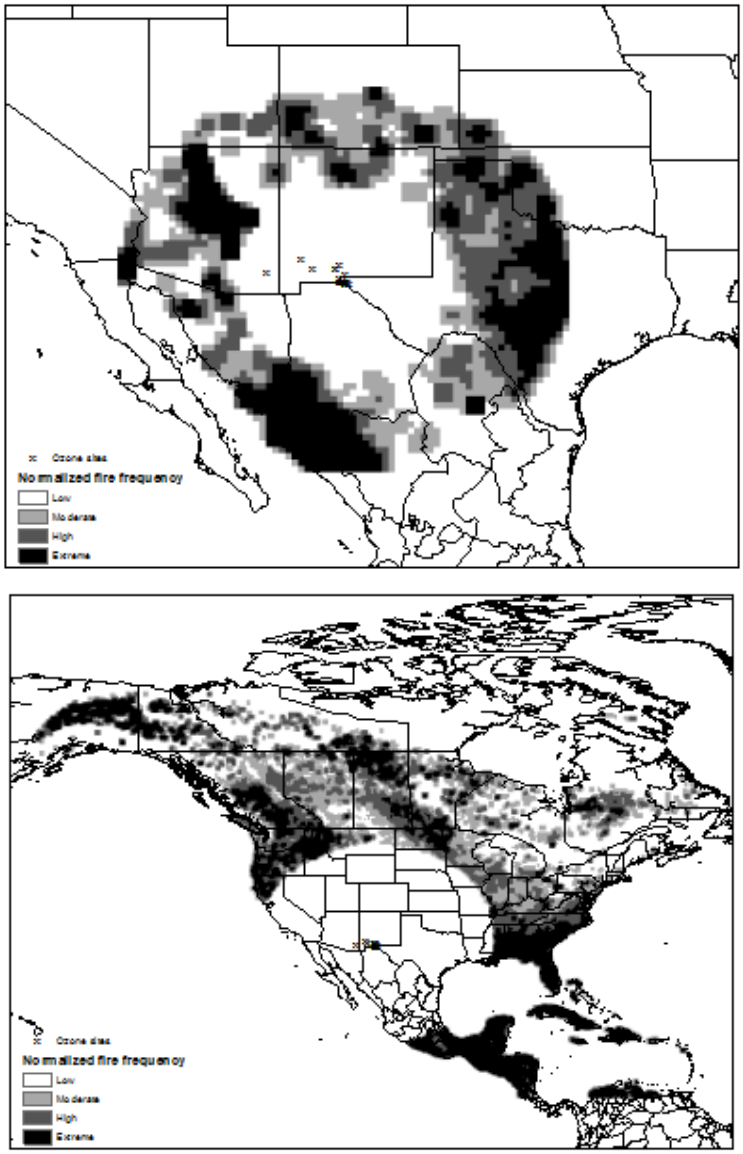

Figure 2.4-2. Spatial variation of MODIS fire detections within the 250-500 miles (a) and 1000-3000 miles buffer zones for sites in Sunland Park, El Paso and Ciudad Juarez region.

The monthly variation of fire detections in the 250-500 miles and 1000-3000 miles buffer zones demonstrated a prevalence of fires in spring for the 250-500 miles buffer zone, and a bimodal distribution in early spring (March-April) and summer (July-August) for the 1000-3000 buffer zone (Figure 2.4-3). The observed patterns of fires and air masses origin indicated that regional

fire events in northwestern Mexico southeast US and Caribbean islands may be responsible for elevated O_3 concentrations in southern NM and El Paso region.

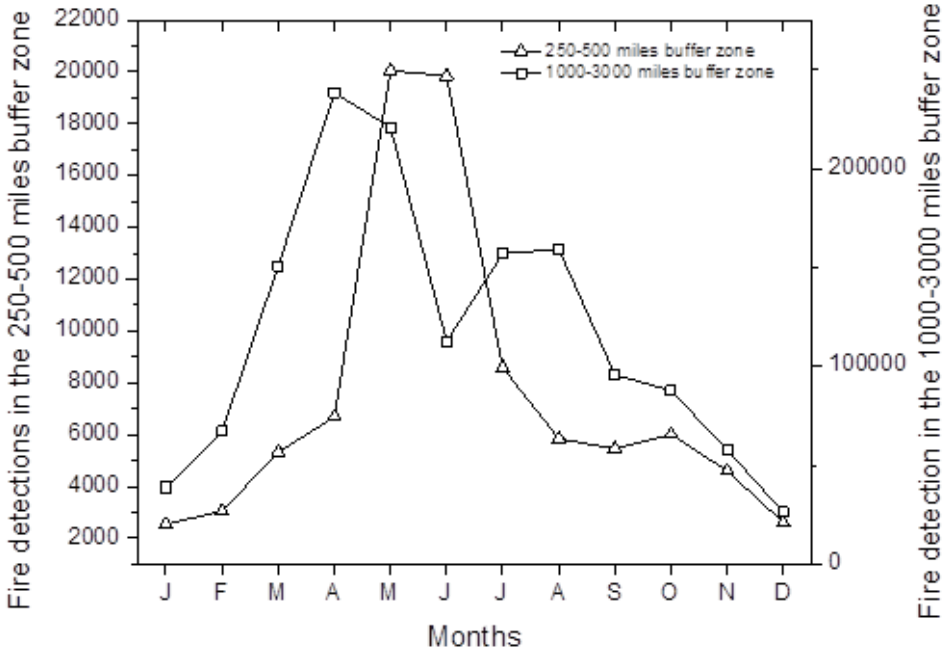

Figure 2.4-3. Monthly variation of MODIS fires detections in the 250-500 miles and 1000-3000 miles buffer zones for sites in Sunland Park, El Paso and Ciudad Juarez.

2.5. Asthma and COPD Hospitalizations

The contribution of wildfires on 8-hr O_3 concentrations are comparable and/or higher than the increases of O_3 levels for which statistically significant relative risks of mortality, hospital admissions and emergency room visits were estimated. Anderson et al. (2004) reported a relative risk of 1.003 (95% CI=1.001-1.004) for a 10 µg/m^3 (5.1 ppbv) change in 8-hr ozone concentration in Europe. Statistically significant relationships between elevated O_3 concentrations and visits to emergency departments for asthma (Tolbert et al., 2000; Mar and Koenig, 2009) and hospital admissions for respiratory diseases (Thurston and Ito, 2001; Ji et al., 2011) have been reported. Romieu et al., (2003) indicated an increase of 27% in the risk of lower respiratory infections for an increase of 20 ppbv of 8-hr O_3 concentration in Ciudad Juarez, Mexico. The California Air Resources Board estimated that for an increase of 10 ppb of 8-hr O_3 concentration above 70 ppb, premature mortality and hospital admissions for respiratory diseases would increase by 600 and 3600 incidents per year, respectively. Similarly, for children, the emergency room visits for asthma would increase by 180 cases per year and a total of 2.6 million days would be lost.

The number of asthma and COPD hospitalizations for children and adults that is associated with the mean and maximum contributions of wildfires on O_3 concentrations were computed using an exposure risk coefficient for asthma and COPD and county-based hospitalization discharge data for the New Mexico counties (Sheffield et al., 2011). The exposure risk coefficient was computed, as follows

where β is related to an increase of 4.25% (asthma,all ages), 1.85% (asthma, children), 2.46 (asthma 15-64 years) and 3.29% (COPD, all ages) for 1n increase of 10 ppbv of 8-hr maximum O_3 concentration (Ji et al., 2011). Because of the good temporal and spatial correlations of O_3 concentrations among the sites in New Mexico, we assumed an average contribution of 5.2 ppbv (and a maximum of 8 ppbv) on 8-hr maximum ozone concentration from wildfires.

Table 2.5-1 Percentage of asthma and COPD hospitalizations in 2010 due to wildfire related O_3 (mean and maximum contributions)

County	Mean contribution ΔO_3=5.2 ppbv	Maximum contribution ΔO_3=8 ppbv
Asthma (All Ages)	2.19	3.29
Asthma (Children)	0.97	1.49
Asthma (15-64 ages)	1.29	1.99
COPD (All ages)	1.72	2.66

The contribution of wildfires-related O_3 on annual asthma hospital admissions were 0.97% (1.49% maximum) for children, 1.29% (1.99% maximum) for adults ages 15-64 and 2.19% (3.39% maximum) for adults all ages. This trend provided an indication that older adults are more susceptible to short-term elevated exposures to O_3. For COPR, the annual mean hospitalizations due to wildfire-related O_3 were 1.72% (2.66%). It is noteworthy that these estimates are based on the annual asthma hospitalizations that include periods of allergens-induced asthma hospitalizations in spring while wildfires in this region are observed in the summer (Figure 2.4-3). Thus, they represent a rather conservative but still significant estimate of the effects of wildfires on health.

2.6. Conclusions

Hourly O_3 concentrations for 23 sites in southeastern Arizona, southwestern New Mexico, El Paso and Ciudad Juarez for the 1993-2010 period were retrieved from EPA AQS. The monthly 8-hr maximum concentrations were calculated to evaluate the annual trends and the impact of wildfires on O_3 pollution. For monitoring sites located in urban and rural populated areas, the monthly 8-hr maximum O_3 concentrations have been declining from 0.15 up to 1.22 ppbv/yr due to reduction in emissions of O_3 precursors in urban communities. On the contrary, O_3

concentrations in Chiricahua demonstrated a statistically significant increasing trend. The moderate correlations between urban sites and Chiricahua site indicated that there were substantial differences between urban and background sites. These discrepancies may be partially attributed to the increasing frequencies and intensities of wildfires. Significant associations among monthly 8-hr maximum concentrations and the frequency of fires were computed for fire incidents in six buffer zones (< 100, 100-250, 250-500, 500-1000, 1000-2000 and 2000-3000 miles).

Overall, a net contribution of up to 10 ppbv on monthly 8-hr maximum O_3 concentrations were computed. Fires within 250 miles triggered a reduction of 8-hr maximum O_3 concentrations as high as 13 ppbv in urban sites. This was attributed to changes on the relative importance of VOC and NOx mixtures as increased fire-related VOCs emissions were combined with urban VOC/NOx mixtures. Strong positive contributions (up to 19 ppbv) were computed for fires incidents at more than 500 miles. This was attributed to the formation of O_3 in smoke plume during transport and its mixing with ground-level air. Fires in western Mexico, southeast US and Caribbean islands may be responsible for a fraction of the observed contributions. The increase of 8-hr maximum O_3 concentration due to regional wildfires was responsible for an increase from 0.97% to 3.39% for asthma and/or COPD annual hospitalizations.

3. Analysis of Historical PM_{10} and $PM_{2.5}$ in the Study Region

High wind and blowing dust storms are a common feature of the study area due to the arid climate, weather conditions and plentiful dust sources in the Chihuahuan Desert. These storms occur more frequently during late winter and the spring, but blowing dust has caused exceedances at all times of the year. Controlling these natural events and emission sources is impractical due to the feasibility and cost effectiveness of implementing control measures.

3.1. Daily PM_{10} Concentrations

PM_{10} concentrations show a marked temporal pattern in the region. By grouping PM_{10} exceedances by season, the spring months clearly have the most exceedances (Figure 3.1-1). The summer season shows the second most exceedances because data from the first half of June, which is technically spring, is included in the calculation.

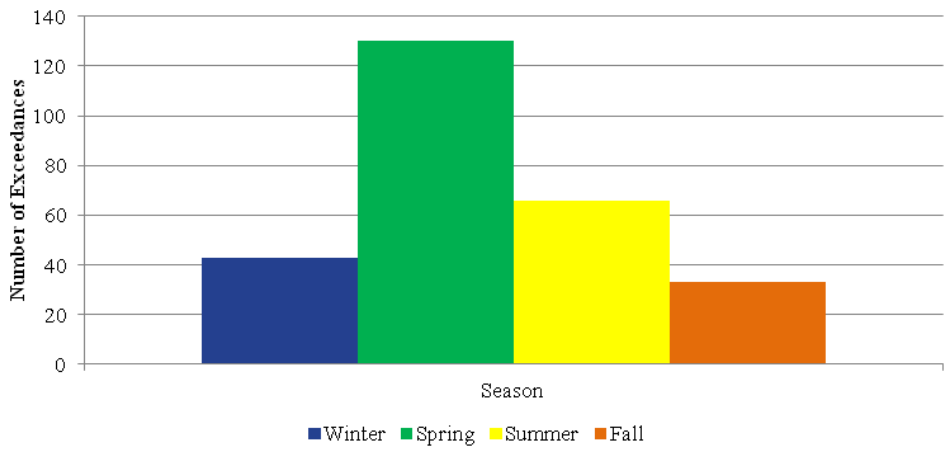

Figure 3.1-1. Number of PM_{10} 24-hour averages exceeding the NAAQS in New Mexico during the years 2003 to 2009. Winter = December, January, and February. Spring = March, April and May. Summer = June, July and August. Fall = September, October and November.

Only 2 percent of days have 24-hour averages that exceed the NAAQS of 150 at monitoring sites in the Paso del Norte. Monitors located in the Paso del Norte airbasin (Anthony, Chaparral, Desert View and SPCY) show slightly higher 24-hour PM_{10} averages than the monitors in Las Cruces and Deming.

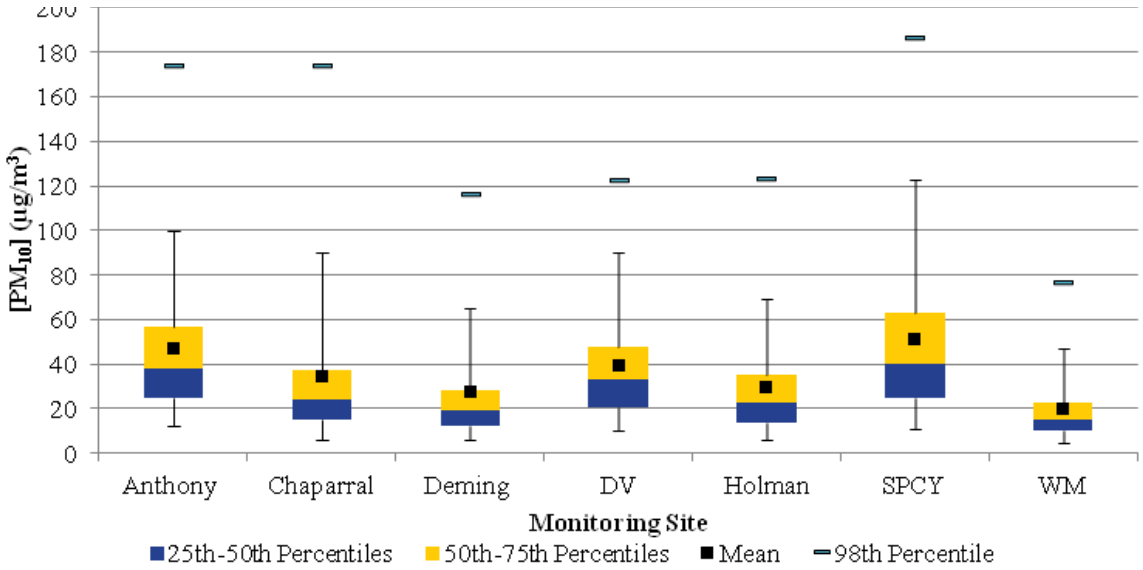

Figure 3.1-2. 24-hour average PM_{10} data distribution in southern New Mexico. The top whisker represents the 95th percentile while the bottom whisker represents the 5th percentile. DV=Sunland Park Desert View, WM=Las Cruces West Mesa

When high wind blowing dust events are excluded from the data set, a marked decrease in 24-hour PM_{10} averages can be seen (Figure 3.1-3).

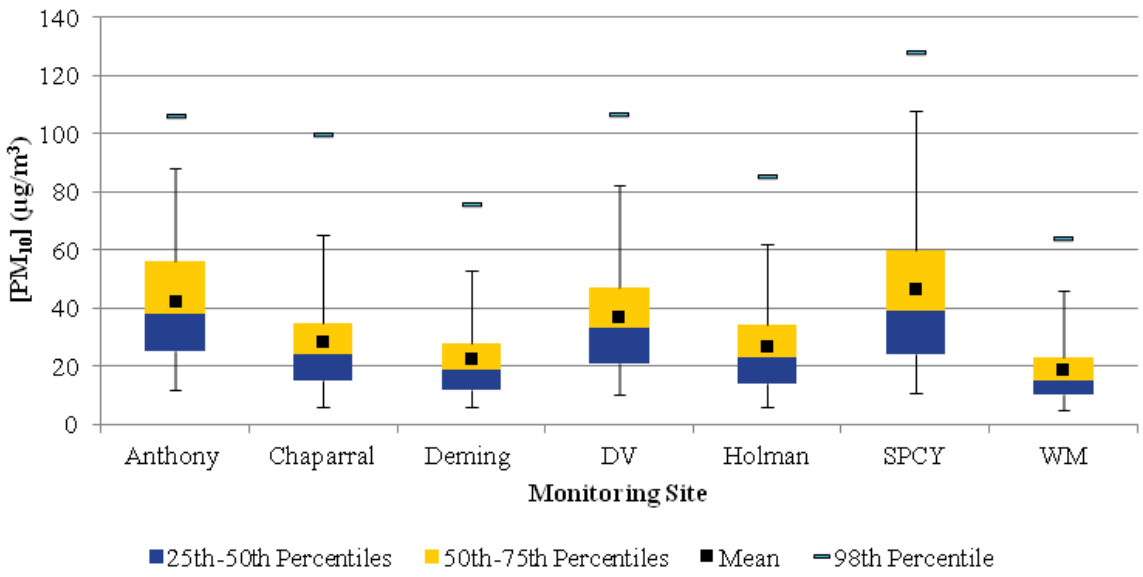

Figure 3.1-3. Daily PM_{10} excluding high wind events. DV=Sunland Park Desert View, WM=Las Cruces West Mesa

3.2. Hourly PM_{10} Concentrations

A clear diurnal pattern also emerges when using hourly data to create box and whisker plots. From Figures 3.2-1 to 3.2-7, the highest hourly PM_{10} concentrations occur in the late morning and early evening. In the PdN airshed, noticeable peaks can also be seen in the early morning and evening hours. This coincides with peak traffic flow as people are going to and returning from work. Numerous unpaved roads in Cd. Juárez are the suspected primary emission sources.

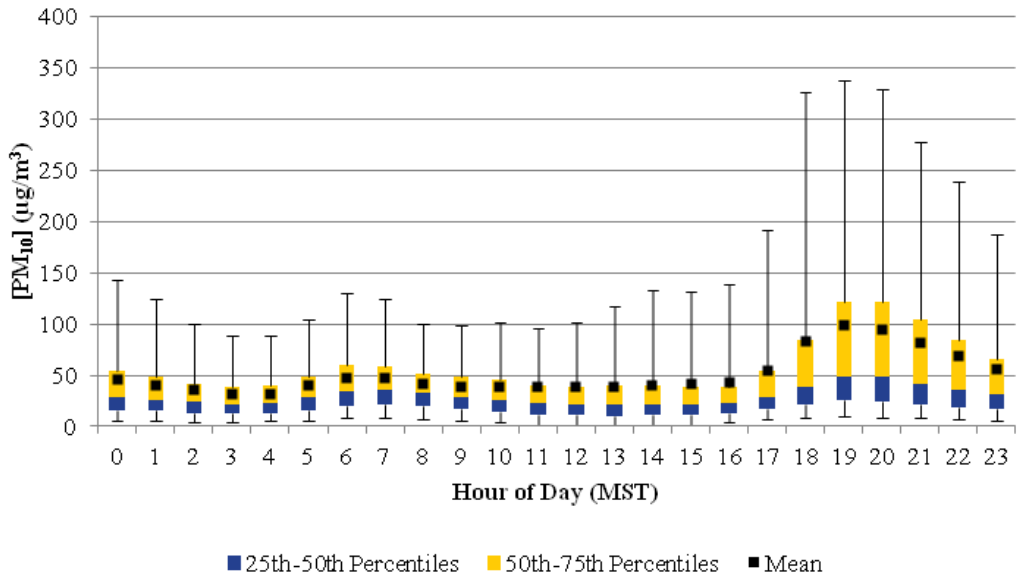

Figure 3.2-1. Sunland Park City Yard (SPCY) hourly PM_{10} for all days

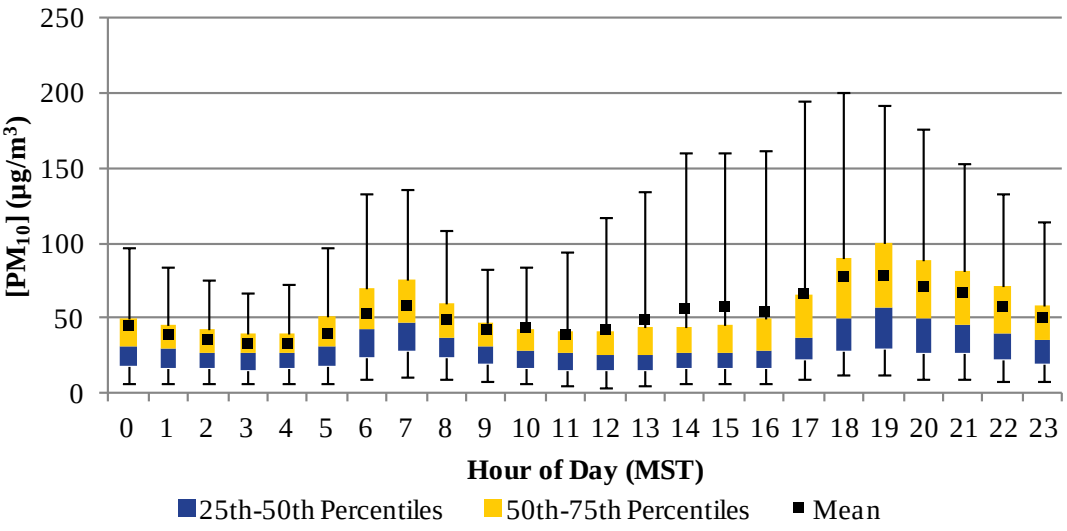

Figure 3.2-2. Anthony Elementary hourly PM_{10} for all days

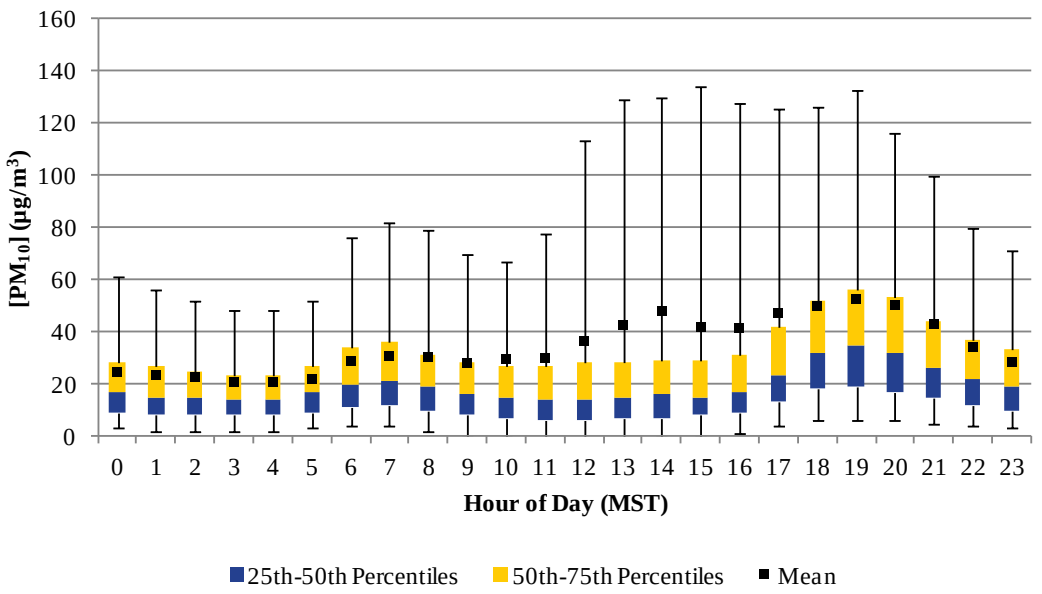

Figure 3.2-3. Chaparral hourly PM_{10} data for all days

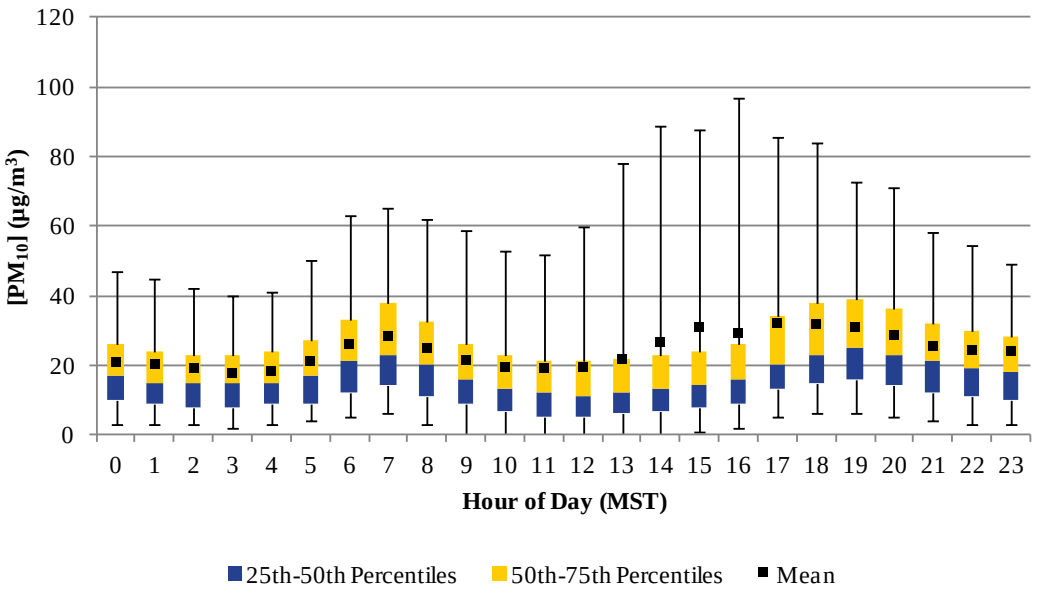

Figure 3.2-4. Deming Airport hourly PM_{10} data for all hours

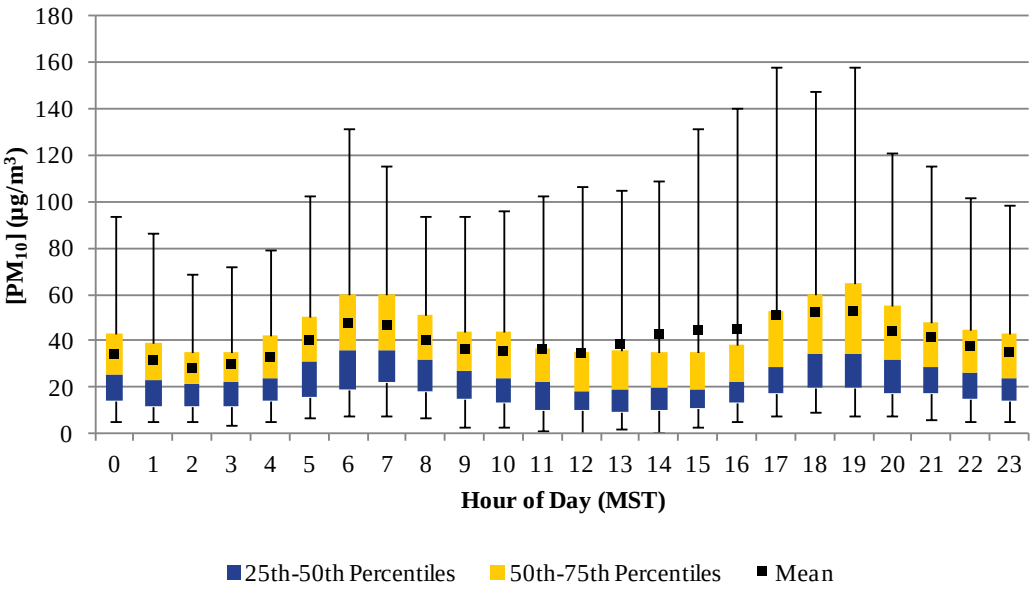

Figure 3.2-5. Sunland Park Desert View Elementary hourly PM_{10} for all days

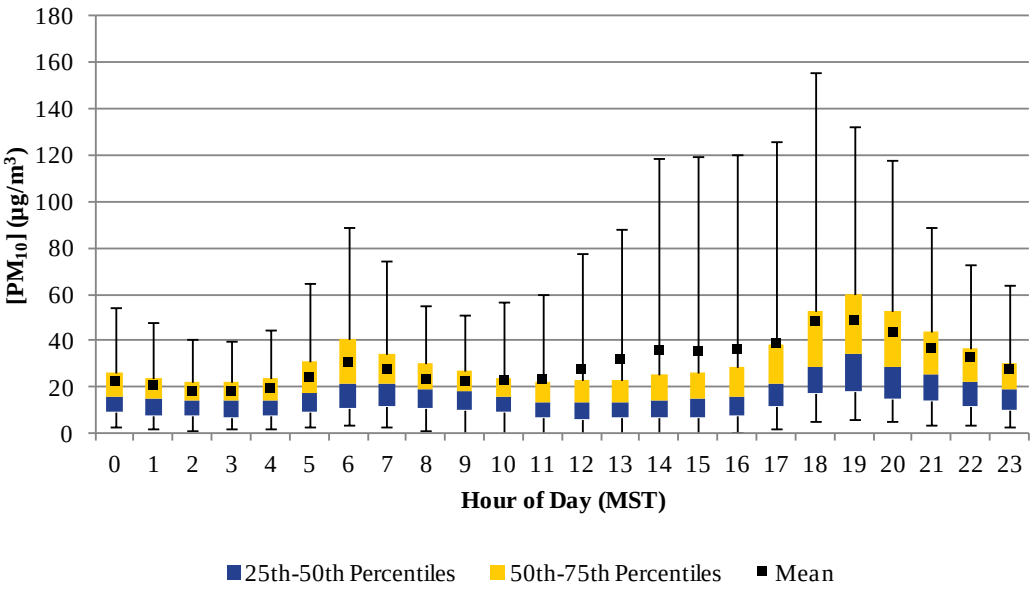

Figure 3.2-6.Las Cruces Holman Road hourly PM_{10} for all days

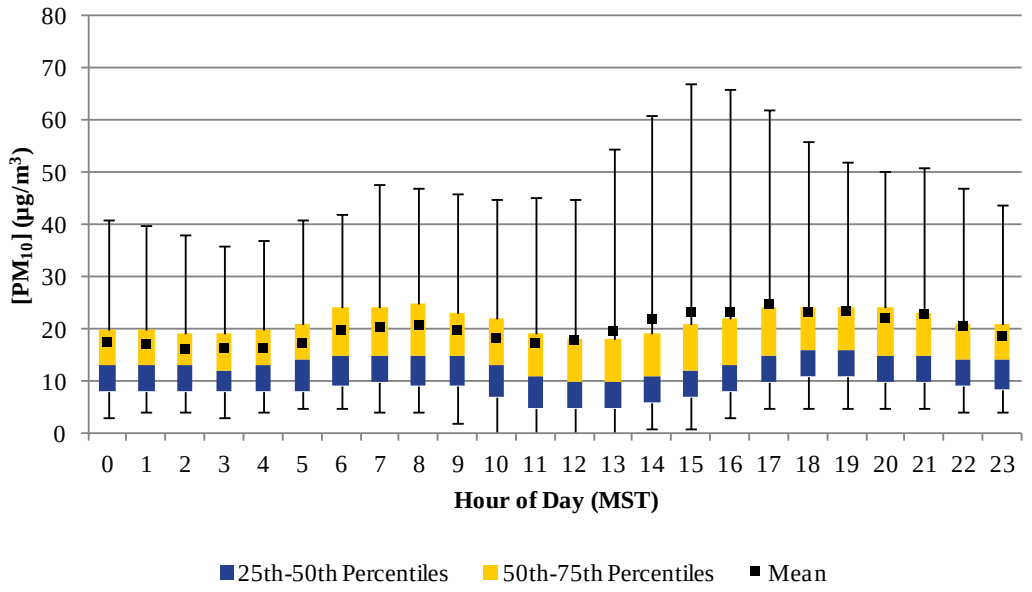

Figure 3.2-7. Las Cruces West Mesa hourly PM_{10} for all days

During high wind blowing dust episodes, daytime heating of the earth's surface causes instable air masses near the surface. When combined with strong winds caused by cold fronts and outflow winds from thunderstorms, the potential for windblown dust increases. An examination of hourly PM_{10} concentrations during these events shows routine exceedances of the NAAQS with some values reaching into the thousands of $\mu g/m^3$. For some of these events, a few hourly values will be high enough by themselves to cause an exceedance of the standard. In figures 3.2-8 and 3.2-9, we can still see the morning and evening peak but the early morning to late afternoon hourly values drop dramatically compared to figures 3.2-1 and 3.2-2.

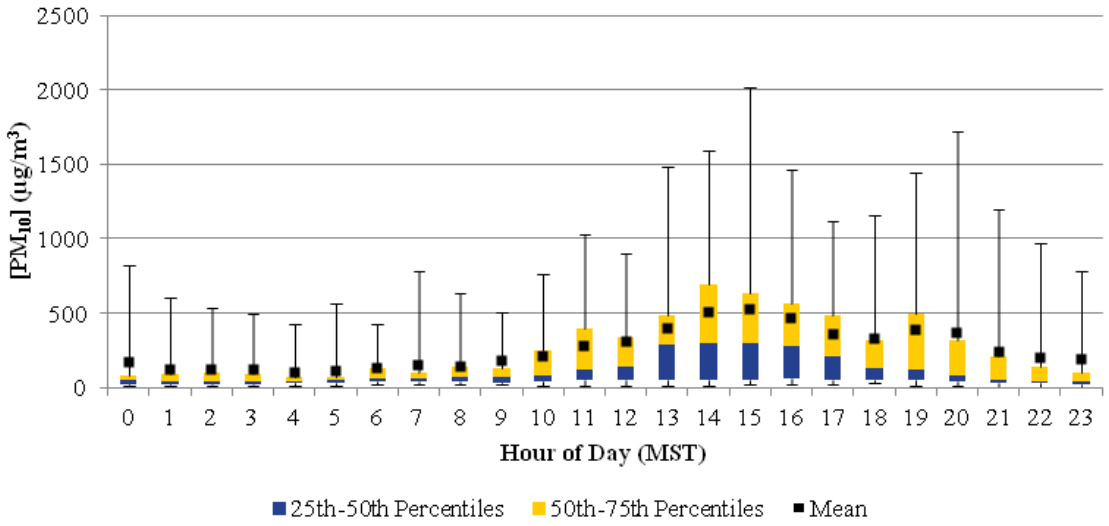

Figure 3.2-8. Sunland Park City Yard hourly PM_{10} during exceedance days

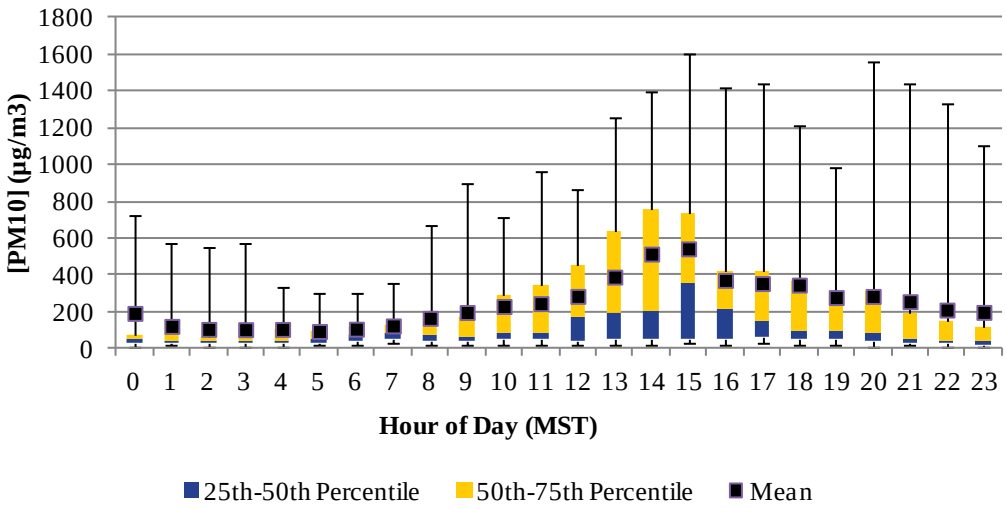

Figure 3.2-9. Anthony Elementary hourly PM_{10} during exceedance days

3.3. Historical $PM_{2.5}$

Exceedances of the $PM_{2.5}$ NAAQS are also caused by regional dust storms but are also monitored in the Paso del Norte airshed when wind speeds are low (≤ 2 m/s) during the winter. Strong to moderate atmospheric inversions and light surface winds limit vertical and horizontal mixing during this time period, causing pollutants to buildup. Incomplete combustion from heating and cooking fuel, as well as unpaved roads contribute to these high monitored

concentrations. $PM_{2.5}$ levels have been shown in past studies to make up from 10 to as much as 30 percent of PM_{10} from dust.

3.4. Daily $PM_{2.5}$ Concentrations

$PM_{2.5}$ levels are highest during the winter and tend to drop off the rest of the year except for days with windblown dust. The number of monitored exceedances ranged from zero in 2009 to a high of 10 in 2011.

3.5. Hourly $PM_{2.5}$ Concentrations

An analysis of hourly $PM_{2.5}$ data shows peak concentrations around dawn and dusk (Figure 3.5-1 through 3.5-4). In the morning people are preparing for and leaving to work when temperature inversions are still in place. As the sun rises and heats the earth's surface the inversion begins to break, allowing for better mixing and transport of pollutants. In the evening people return home and turn up heating devices and cook dinner as an inversion begins to form. Traveling on unpaved roads during both time periods also contributes to increased emissions. It should be noted that the TEOM monitoring method used to collect hourly $PM_{2.5}$ data are not approved by EPA for comparison to the NAAQS and the data collected is for informational purposes to track trends and provide the public current and forecasted air quality conditions.

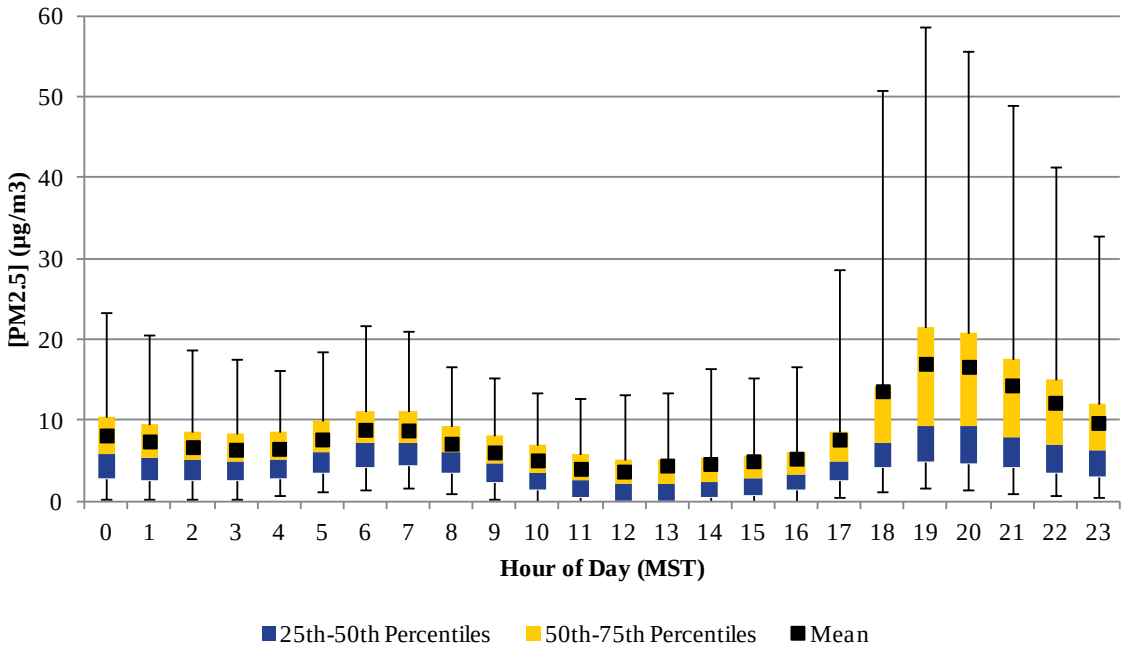

Figure 3.5-1. Sunland Park City Yard hourly $PM_{2.5}$

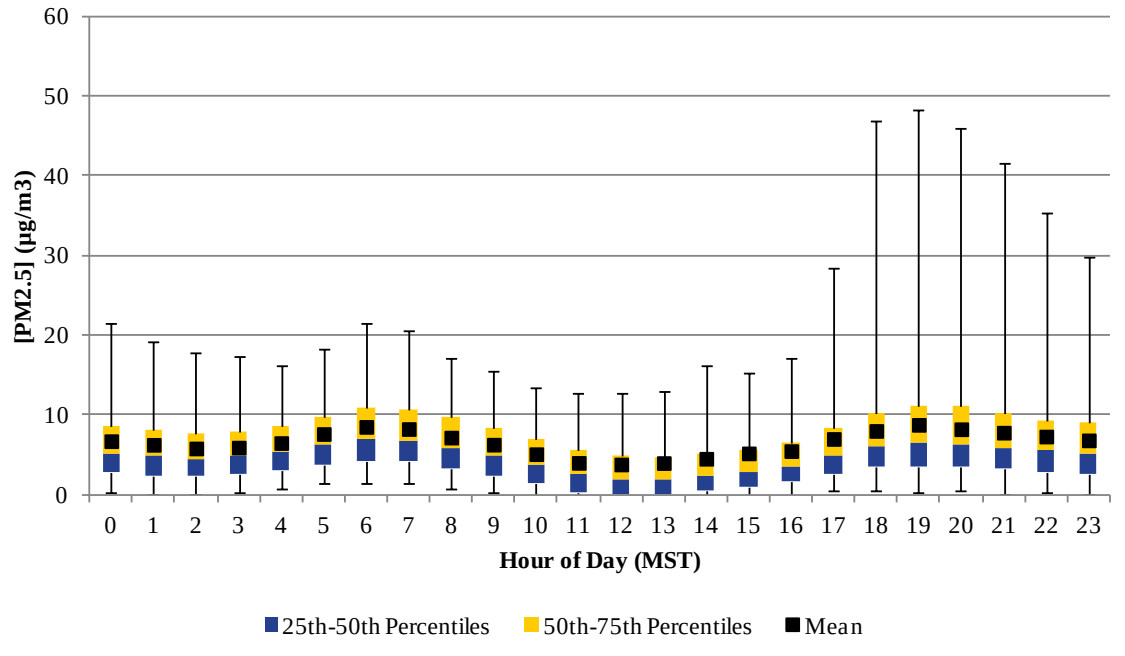

Figure 3.5-2. Sunland Park Desert View Elementary hourly $PM_{2.5}$

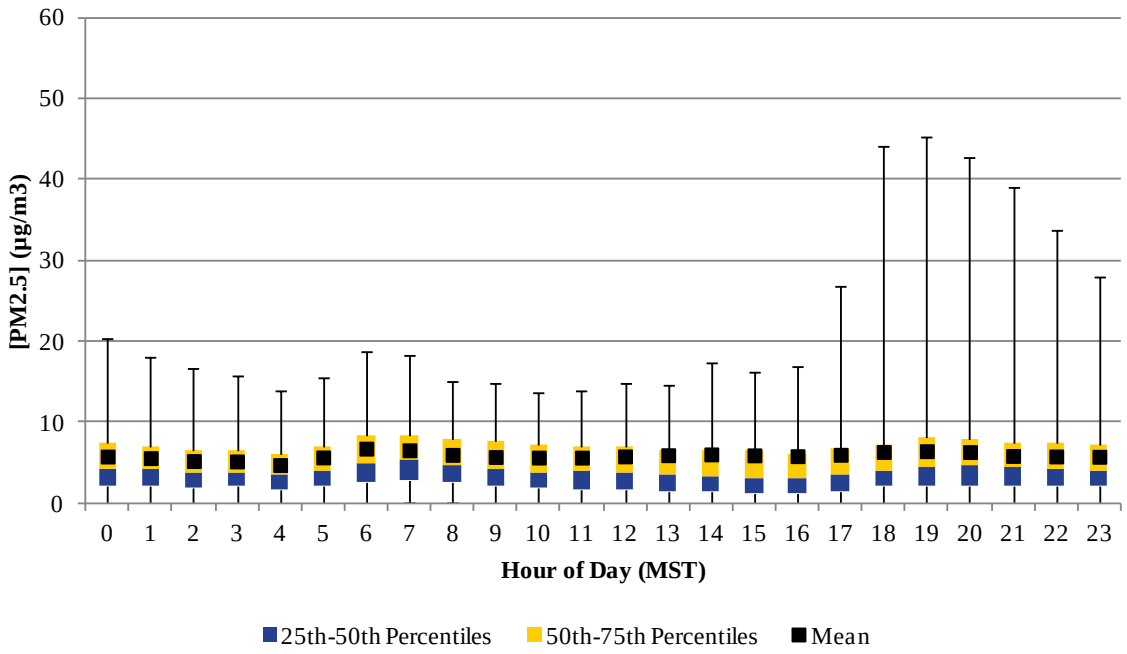

Figure 3.5-3. Santa Teresa Port of Entry hourly $PM_{2.5}$

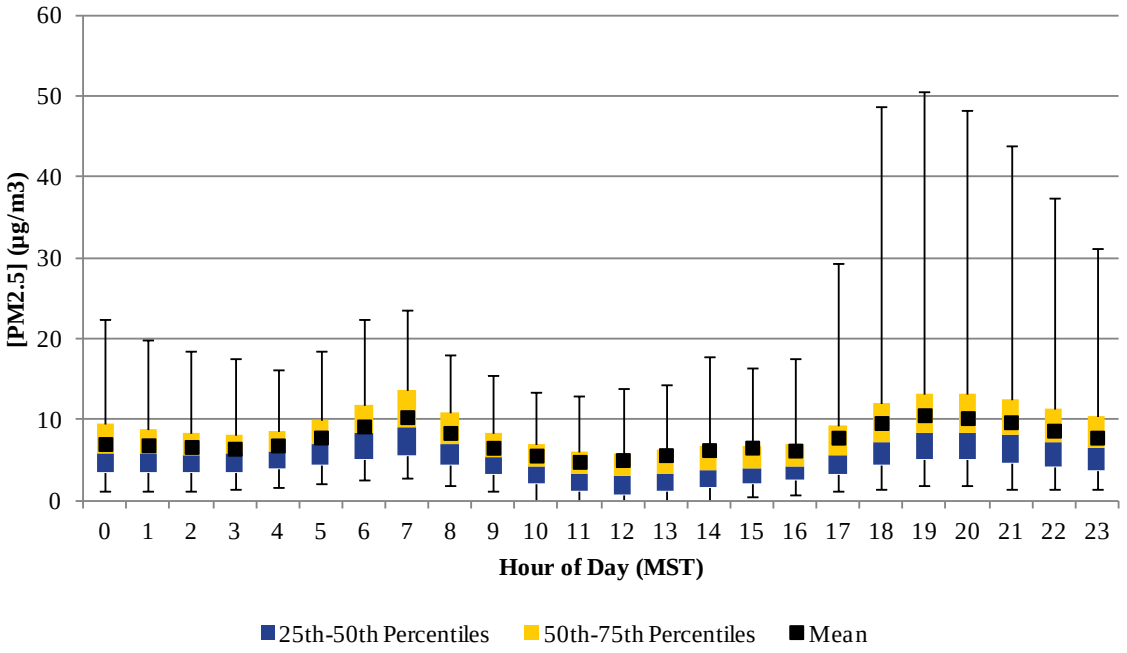

Figure 3.5-4. Anthony Elementary School hourly $PM_{2.5}$

3.6. Annual $PM_{2.5}$ Concentrations

Unlike PM_{10}, EPA also sets an annual NAAQS to protect public health from chronic exposure to $PM_{2.5}$. The annual standard is much lower than the daily standard set by EPA. Figure 7 provides the annual arithmetic mean of $PM_{2.5}$ concentrations in El Paso, TX, Sunland Park, NM and Las Cruces, NM.

4. Remote sensing of regional dust events for population exposure

4.1. Dust Event Archive:

As of this point in time, we have identified 442 days during the period April 18, 2000 to May 2, 2012 for which we have determined that there is a dust event. In some cases, the event stretches across more than 1 day. In most all cases, a dust event is classified as a period during which a dust plume has been identified in satellite imagery in New Mexico or in the region surrounding New Mexico. Those locations in this surrounding region where most events are observed are four corners (NE Arizona and NW New Mexico), southern Colorado, panhandle of Texas, northern Chihuahua, and Northern Sonora. A very small number of these 442 events are somewhat outside our region in central Mexico, Nevada, and Utah.

The archive stands at about 1.1 TB currently and is growing daily as we continue to add MODIS and AVHRR, and eventually, more GOES data as well as to add new events. In addition, as reported in the next section, as we identify possible dates prior to 2000 for which there may be a dust event, we can carry the satellite archive back to approximately 1980. This would give us a 30-year period over which we can determine locations of dust emissions as well as extent of plume coverage.

4.2. History of Dust Events:

Two efforts that are on-going are meant to determine the extent of dust events in the past (possibly going back until the late 1800s). The first of these is to scan journal articles from the archives of the American Meteorological Society for “dust events”. The initial inventory of articles was determined by using keywords such as “dust”, “sand”, “wind”, etc. while searching the AMS journal archive. Those articles that seemed likely to be of interest were downloaded and are being “visually scanned” for more specific information.

The second effort is to “scan” the National Weather Service archive of weather/climate data for “dust events”, “haze events” and “high wind events”. The source of these data is the archive of the COOP weather reports as summaries of the day. In some instances the COOP stations use

the option of reporting "significant weather events" of which the above three are among several other event types. For the states of Arizona, Utah, Colorado, New Mexico, Texas, Oklahoma and several others, dates for which these events occurred along with the geographic location of the reporting station were noted and recorded as text files. The CD-ROM from which these data came covers the period from the late 1800s to 2000 -- it may be that reporting of significant events was not possible during this whole period and this is something that remains to be determined. We have nearly finished processing the period from 2001-2011.

The significant weather events along with the events noted from the journal articles will provide a basis for searching the satellite archive back to 1980 and for the period before that, some idea of the spatial extent and frequency of events. Perhaps, the extent of reports from these data can be "correlated" to our current archive to infer a more extensive estimate of past actual events.

4.3. Air Quality Monitoring/Forecasting/Simulation:

We have acquired two air quality/dust models; both of which couple to our WRF model. The first of these is CHIMERE (http://www.lmd.polytechnique.fr/chimere/), a chemistry transport model for air quality forecasting and simulation. CHIMERE has been installed on our multi-processor server and now needs to be made operational. The other model is the DREAM model (http://www.bsc.es/projects/earthscience/BSC-DREAM/). It remains for DREAM to be installed and to then exercise to an operational functionality.

4.4. Landsat Data Archive:

We have downloaded the Landsat data (Landsat 4, 5, 7) in its entirety (~1985 to present) for the "border region" during FY12. The Landsat data, at a spatial resolution of 30m, will provide detailed information for those regions responsible for the dust emissions as well as possible precursors for dust source activation (e.g.; removal of vegetation, etc.). The archive consists of compressed tar files that need to be uncompressed and untarred before being processed to calibrated data. We already have in place the necessary software for accomplishing this task as a batch process; we now need to make it happen.

5. Palomas-Columbus PM_{10} Study

The Palomas-Columbus study was a collaboration between the current NM DOH research effort and a Chihuahua Rural Task Force and US EPA Border 2012 project lead by Erin Ward. The study region includes the border communities of Columbus and Palomas in southern New Mexico.

East to west, it covers an expanse of 4 kilometers and north to south it covers approximately 7 kilometers. This area is characterized by a small population, highly variable PM concentrations, and a very limited record of compliance measurements for PM_{10}.

The Palomas PM_{10} study described in this program plan is needed to provide information on the sources and levels of PM_{10} in and around the northern border and the cattle holding facilities. The objectives of this study are:

- To acquire a database of particulates and environmental conditions with specified precision, accuracy, and validity which is suitable to determine contributions of elevated PM_{10} concentrations
- To estimate the spatial and temporal distributions of PM_{10} concentrations, especially near fugitive dust sources.
- To estimate fugitive dust contributions based on existing PM_{10} emissions information

5.1. Aerosol and Meteorological Monitoring Network

The focus of the ambient aerosol and meteorological measurement network was on collecting data to help understand the impacts of fugitive dust sources such as the cattle facility and unpaved roads in and around Palomas. To do this we installed and operated a small network of aerosol samplers in northern Palomas surrounding the cattle facility over a period of a month. Sample collection began on March 28, 2012 and end on April 29, 2012.

The measurements were collected using a combination of 24-hour integrated filter samples and continuous sampling. One of the samplers collected PM_{10} with an EPA Federal Reference Method while the remaining were non-reference methods. The filter samplers were analyzed for total mass concentration to be compared to the 24-hour National Ambient Air Quality Standard. The increased time resolution provided by the continuous or real-time measurements enabled examination of brief spikes in pollutant concentrations from the various fugitive dust sources in Palomas and Columbus.

The Palomas monitoring network was designed to provide samplers on all sides of the cattle facility. A sampler located on the west side of Palomas was used as an upwind station when the winds are blowing from the west to southwest directions. Wind transport directions will be logged at one station downwind of the cattle facility. Two monitoring stations were installed on the US side of the border in Columbus to address particulates north of Palomas. Another station in the town of Columbus also operated during part of the study. Figure 5.1-1 shows the Palomas monitoring site map centered around the cattle facility.

The Palomas monitoring network was augmented with the NM Department of Health satellite station in Columbus and two MetOne E-BAM PM_{10} monitors on loan from the New Mexico Environment Department Air Quality Bureau. A MetOne particle sizer was operated at the NM Department of Health satellite monitoring station as part of its normal operation. This site is located in the backyard of Martha's Bed and Breakfast, on the southeast side of Columbus. A meteorological station is located at this site collecting wind data at 3-meters, temperature and RH at 1.5-meters, along with precipitation, and solar radiation.

The table below summarizes the study monitoring network and instrumentation at each monitoring site

Site ID	**Network**	**Location**	**Instruments**
PRIN	Palomas	In front of house of Principal Jose Luis east of cattle facility in Palomas	Minivol PM_{10} with Teflon filter
CTSE	Palomas	Mireya Perez's house southeast of the cattle facility; instruments were mounted on the east end of the roof at 3 meters above the ground	MetOne Profiler 212 particle sizer Davis VantagePro2 weather station
CTNE	Palomas	Northeast corner of cattle facility in Palomas	Minivol PM_{10} with Teflon filter (DRI) Minivol PM_{10} with quartz filter (DRI)
CTSW	Palomas	West of cattle facility in Palomas	Minivol PM_{10} with Teflon filter
CTSO	Palomas	South of cattle facility in Palomas	Minivol PM_{10} with Teflon filter
FORD	Palomas	Ford School in western portion of Palomas	Minivol PM_{10} with Teflon filter
CTNO	Columbus	North of cattle facility in Luna County, NM lot	BGI PQ100 PM_{10} with Teflon filter Hourly E-BAM PM_{10}
CPOE	Columbus	US Port of Entry, in east parking lot behind office complex	Hourly E-BAM PM_{10}

Site ID	Network	Location	Instruments
MTPL	Columbus	NM DOH satellite site at Martha's Place Bed & Breakfast	3-meter meteorological station MetOne model 212 profiler particle sizer

The following map (Figure 5.1-1) shows the location of the monitoring site with their corresponding site identifications. The site CTD1 and CTD3 were to be used by Dr. Margez for collecting data with the TSI DustTrack instruments during windy days. Unfortunately, he was not able to conduct sampling on the two days with highest wind due to scheduling conflicts. Data was also lost after his laptop was stolen in a robbery soon after the study.

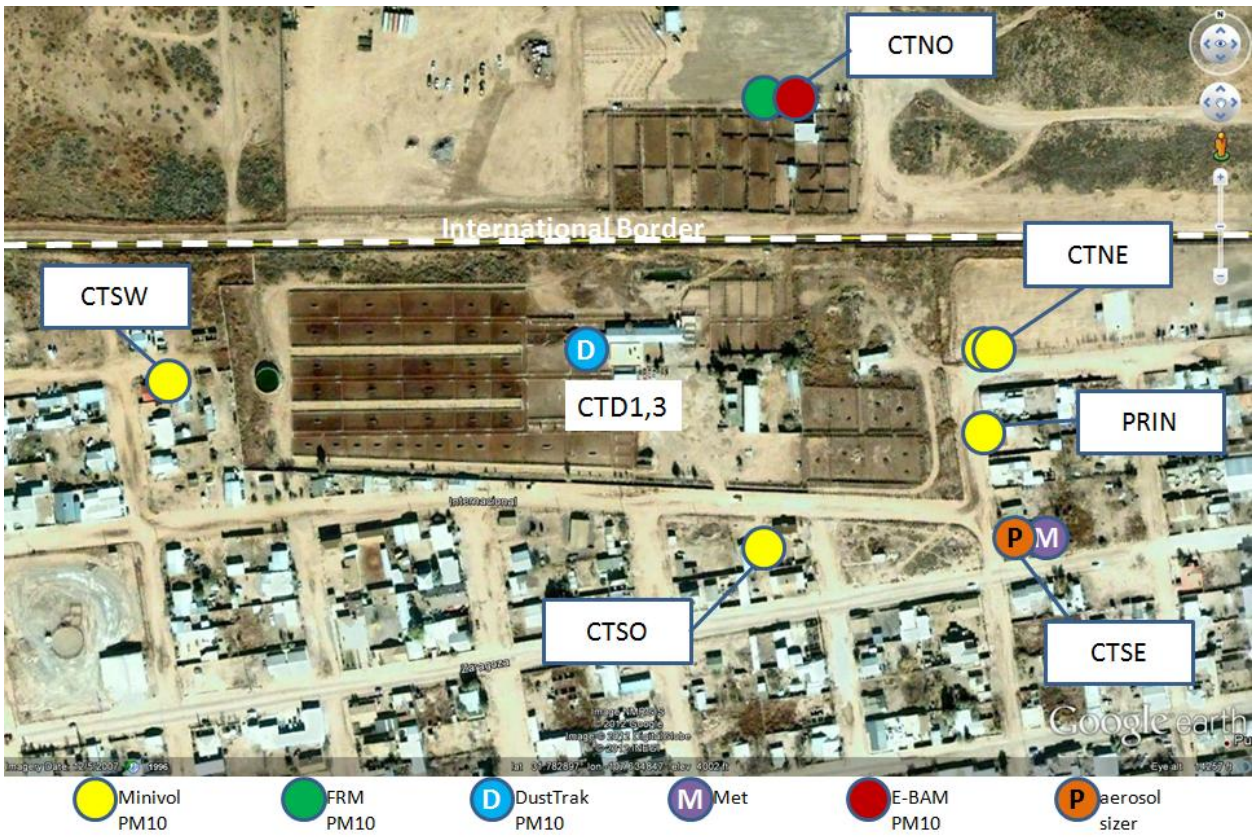

Figure 5.1-1. Monitoring network surrounding the cattle facility with site IDs

Figure 5.1-2 shows the general location of the all of monitoring stations including those in Columbus.

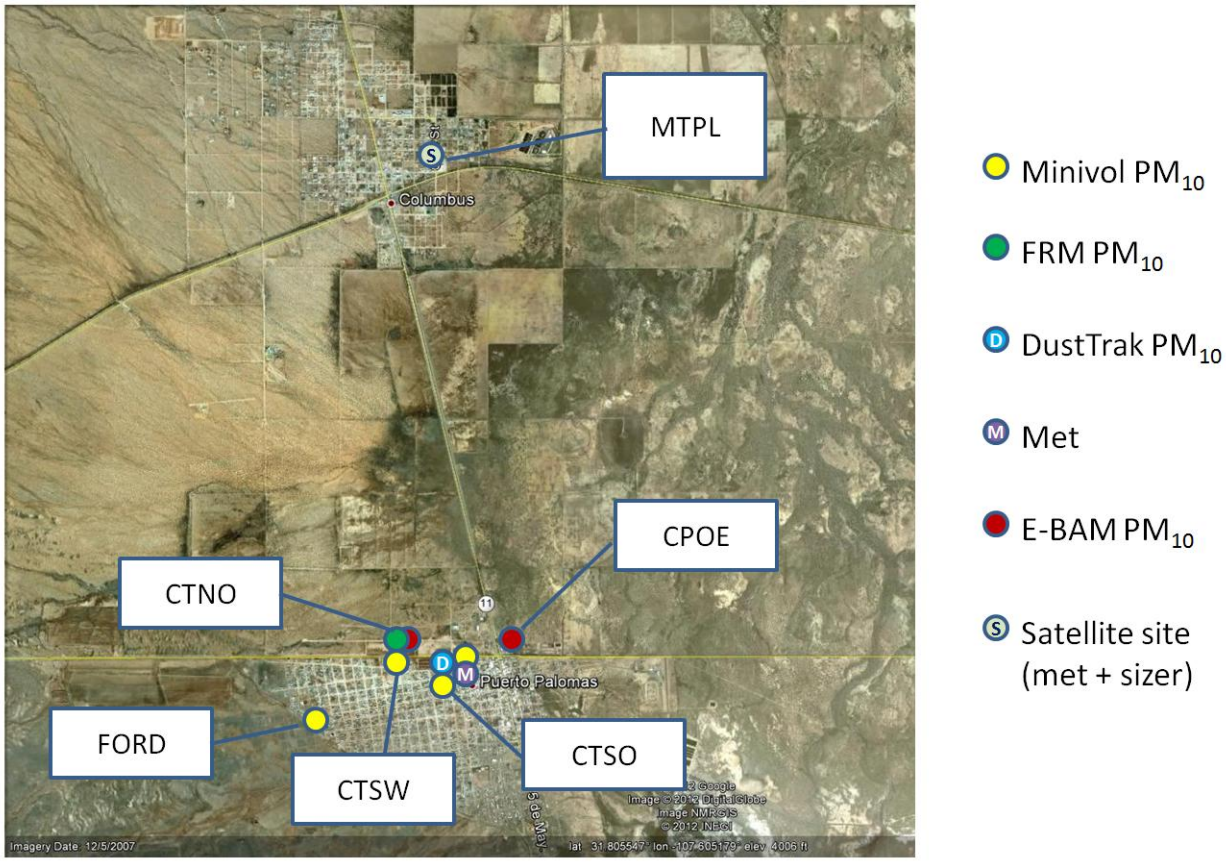

Figure 5.1-2. Regional monitoring network

5.2. Ambient Aerosol Instrumentation

5.2.1. Filter based Measurements

Integrated filter samples were collected for 24-hour integrated PM_{10} mass concentrations using battery powered Airmetrics MiniVol TAS samplers. Four of the units were on loan from the Desert Research Institute and two were from the NM DOH study. These samplers consisted of a pump, timer, tubing and fittings, removable filter holder, flow meter, impactor inlet, and battery pack. We operated the samplers at a constant 5.0 liters per minute (lpm) flow rate during the 24-hour sample. Samples were collected at a height of 3-meters above the ground by attaching to various poles and antennas in Palomas. We used 47 mm diameter Teflon (PTFE) filters that allowed us flexibility in using both gravimetric and light transmission analysis. The PM_{10} samples were collected on filters in numbered filter cassettes, labeled PALXXX. Two removable battery packs accompanied each sampler so that one was charging while the other is being used in sampling. Every time a filter was changed, the discharged batter was replaced with a freshly charged battery.

A BGI PQ100 sampler was used in this study to collect PM_{10} using an EPA Federal Reference Method. The PQ100 used a PM_{10} size selective inlet followed by a 47 mm Teflon (PTFE) filter, at a constant flow rate of 16.7 lpm. The PM_{10} inlet is designed for a 50% collection efficiency for particles of aerodynamic diameter of 10 µm or less at a flow rate of 16.7 lpm. The sampler was equipped to operate from a solar panel charged 12 VDC battery which provides power for a 24-hour sampling period. The PM_{10} samples were collected on filters in numbered filter cassettes, labeled PALXXX. The sampler's air inlet was operated at a height of 1.5-meters above the ground similar to the height of the MetOne E-BAM inlet.

All of the Palomas monitoring stations used Teflon (PTFE) filter substrates since they are durable and can be used to determine the mass concentration, black carbon fraction through light transmission, and potentially elemental composition through XRF or PIXE. These However these filters cannot be analyzed for carbon using the Thermal Optical Reflectance method because of its presence in the filter material, though they have very low blank levels for ions and elements. The primary use of the Teflon filters was in the determination of 24-hour mass concentration using a gravimetric analysis. The filters were weighed at the NMSU Department of Chemistry. A portion of the filters were reweighed at the College of Agriculture Consumer and Environmental Sciences (ACES) soils laboratory for quality checks. Weighing was performed on a Mettler M5 microbalance with +/- 1 µg precision. The balance has a capacity 20 grams, a range of 20 mg on the optical scale and an accuracy of ±0.002 mg. A Cahn-33 microbalance was used to verify the filter tare weights at the Department of Chemistry.

Although not reported in this document, we will also be using a method to evaluate the filter's opacity using a Magee Scientific OT21 dual wavelength (370 nm and 880nm) optical transmissometer thus providing an estimate of the black carbon content. We use this method since carbon cannot be measured directly on the Teflon membrane filters due to presence of carbon in the filter media. This method is also provides a cost savings over the traditional TOR/quartz combination method.

Chemical analysis of the filters collected at the CTNE site, northeast corner of the cattle facility, will be done at the Desert Research Institute's Environmental Analysis Facility. Results of this analysis are also not reported in this document. The Teflon filters will be analyzed using x-ray fluorescence to determine the elemental composition. X-ray fluorescence (XRF) analysis is performed on Teflon membrane filters for Al, Si, P, S, Cl, K, Ca , Ti, V, Cr, Mn, Fe, Co, Ni, Cu, Zn, Ga, As, Se, Br, Rb, Sr, Y, Zr, Mo, Pd, Ag, Cd, In, Sn, Sb, Ba, La, Au, Hg, Tl, Pb, and U with an energy dispersive x-ray fluorescence (EDXRF) analyzer. XRF analyses are performed on a Panalytical Epsilon 5 energy dispersive XRF spectrometer (Almelo, Netherlands). The quartz filters collected alongside the Teflon samples will be analyzed using the Thermal Optical Reflectance (TOR) method for organic and elemental carbon. This method is based on the principle that

different types of carbon-containing particles are converted to gases under different temperature and oxidation conditions (Chow et al., 1993). The different carbon fractions from TOR are useful for comparison with other methods which are specific to a single definition for organic and elemental carbon.

5.2.2. Continuous Aerosol Measurements

The MetOne E-BAM PM_{10} monitor was used at two locations in the US to collect hourly average PM_{10} mass concentration readings to be compared to the 24-hour integrated samples in Palomas. This time resolution provided information on the variation of PM_{10} over the course of the day and peak concentrations during high wind periods. Procedures were followed according to the manufacturer's guidance and calibration was accomplished manually by means of a Mylar film that represents a specific particulate concentration against which to set the monitor. The monitor maintained an error log with date, time, and type of error. Three BAM instruments were on loan from the New Mexico Environment Department Air Quality Bureau from February 24. 2012 to May 22, 2012. Two were used in the study in Columbus and the third was not used due to a malfunctioning pump.

An Optical Particle Counter was used to measure the real time aerosol size distribution at one location southeast of the cattle facility. A MetOne model 212 Optical Particle Counter measured particle sizes from 0.5 to 10 microns in eight size ranges, taking a sample every 60 seconds. This data will be used to interpret the 24-hour integrated filter samples by indicating the size of the particles and temporal behavior. For example if the majority of particles are large, in the upper size ranges of the instrument, this probably indicates that the area is influenced by dust or other source.

5.3. Meteorological Measurement Instrumentation

The Columbus weather station is part of the NM Department of Health's "Assessment of Land-based Sources of Air Quality Contaminants in the Binational Border Region of Southwestern New Mexico, Northwestern Chihuahua and West Texas" project. This monitoring station is located at Martha's Bed and Breakfast at the corner of Lima and Main Street. In the past a NWS Cooperative station was hosted at this location but was discontinued in 2011. The period of record at this location started in August of 1909 and continued till May 2011. The cooperative site identification number is 292024. This site is approximately 380 meters (0.23 miles) northwest of the Pancho Villa State Park. The predominant landuse in the surrounding block is commercial with a few residences located more than a block away. The adjacent streets are paved with some appear to be "chip sealed" but unpaved roads are numerous in the area.

Instrumentation at this site included wind speed and direction at 3 meters, solar radiation, rain rate, and temperature and humidity at 1.5 meters. This site also collects particle size counts from 0.5 to 10.0 microns in 8 size bins. A Campbell Scientific CR1000 data logger acquires data in 5-minute and hourly averages. During summer months this site is capable of collecting ozone using a 2B Technology ozone monitor.

A Davis VantagePro2 meteorological station was used to collect meteorological variables including temperature, humidity, wind speed and wind direction at a location near the southeast corner of the cattle facility in Palomas. The base station provides a wireless connection between the datalogger and the sensor package and was located at the home of Mireya Perez at the corner of Zaragosas and Juventino Rosas Streets. The sensor package was located on a television mast approximately 3 meters above the ground and 1 meter above the height of the roof of the house. To collect data, the data logger was connected to a laptop using a USB cable and the Davis WeatherLink software. The software package will be installed on the laptop PC and be used to store the data in a tabular format. Data was logged in 5-minute intervals during the study.

The following table below describes each sampler type and pollutants collected and sampling interval.

Instrument (# available)	Target Pollutant(s)	Sampling Interval
MiniVol samplers (6)	4 sites with 24-hour PM_{10} mass on 47mm Teflon filter media – to be analyzed for gravimetric mass and elemental carbon 1 site with 24-hour PM_{10} mass on 47mm Teflon and quartz filter media – Gravimetric mass, elements, elemental and organic carbon. On a subset of filters organic speciation using thermal desorption method (TD-GCMS) will be investigated.	Every other day
BGI PQ100 Federal Reference Method sampler (1)	1 site with 24-hour PM_{10} mass on 47mm Teflon filter media to be analyzed for gravimetric mass and elemental carbon	Every other day
Nephelometer (2)	Two continuous PM_{10} DustTrack II instruments operated to give concentration every 60 seconds.	1-minute

Instrument (# available)	Target Pollutant(s)	Sampling Interval
Optical Particle Counter (1)	Continuous aerosol size distribution using MetOne profiler 212 with 8-bin sizes from 0.5 to 10 µm. This will be operated to give size distribution every 5-minutes.	5-minutes
MetOne E-BAM (2)	Hourly PM_{10}, with temperature, relative humidity, and wind speed and direction	1-hour
Meteorological station (1)	The met station will provide continuous temperature, relative humidity, wind speed, wind direction. Averaging time will be set at 5-minutes.	5-minutes

5.4. Temporal and Spatial Variations in PM_{10}

This section presents the descriptive statistics and time series of PM_{10} mass concentrations, particle size measurements, and meteorological conditions collected in the Palomas, Mexico and Columbus, NM areas.

5.4.1. PM_{10} Mass Concentrations

Table 5.4.1-1 summarizes daily PM_{10} along with the mean and median concentrations for all sites during this study. The first four stations are in Palomas, and the bottom three are located in Columbus. This table shows high PM_{10} occurs on both sides of the border and can be observed at the same magnitude.

Table 5.4.1-1 Maximum, Mean, and percentiles of hourly PM_{10} measured at each site. Concentrations are rounded to the nearest µg/m^3 to allow for easier comparison between sites

Site Code	Number of samples	Max PM_{10}	Mean PM_{10}	Median PM_{10}	5th percentile	25th percentile	75th percentile	95th percentile
FORD	15	531	72	29	5	18	56	262
CTSW	16	199	74	69	20	33	95	169
CTSO	16	169	78	75	23	44	98	148
PRIN	15	121	58	40	19	35	82	117
CTNO (filter)	6	305	149	127	54	75	205	283

Site Code	Number of samples	Max PM_{10}	Mean PM_{10}	Median PM_{10}	5th percentile	25th percentile	75th percentile	95th percentile
CTNO (BAM)	51	515	52	35	18	27	52	98
CPOE (BAM)	39	451	45	29	15	22	42	71

Figure 5.4.1-1 shows box plots of 24-hr PM_{10} mass concentration measured at four monitoring sites in Palomas and three monitoring sites in Columbus, NM. The boxes represent the 25%, 50% (median) and 75% percentiles, and whiskers show the 5% and 95% percentiles. The "x" show the 1st and 99th percentile while the "-" denote the maximum and minimum values.

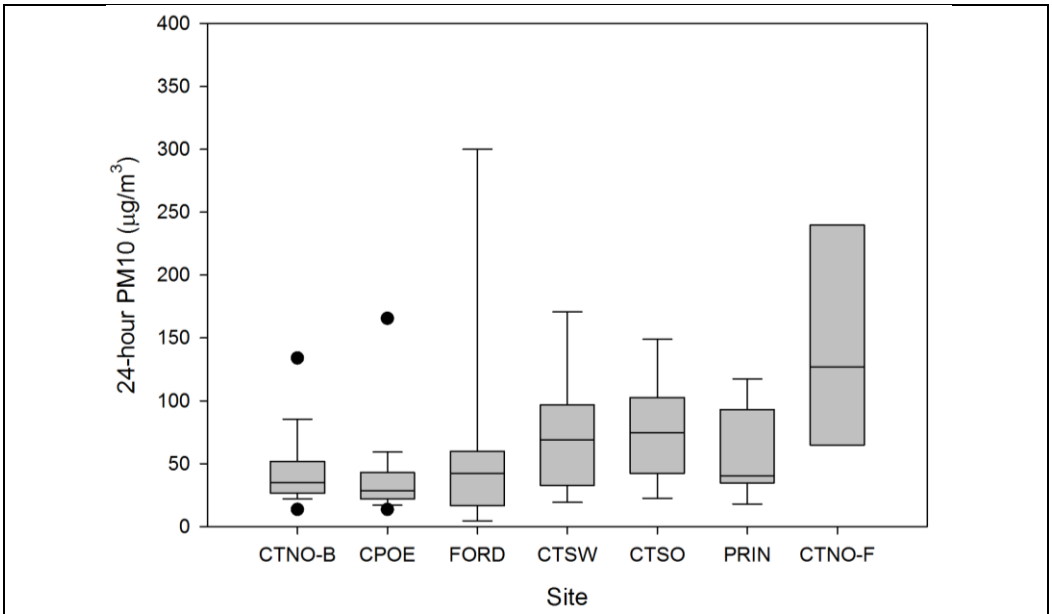

Figure 5.4.1-1. 24-hour PM_{10} mass concentrations.

In Figure 5.4.1-1, CTNO-B refers to the Beta Attenuation Monitor sampling method at the monitoring station and CTNO-F refers to the filter based sampling methodology. Both of the CTNO samplers were situated next to each other.

With respect to the 24-hr PM_{10} National Ambient Air Quality Standard of 150 µg/m^3, PM_{10} levels exceeded the standard at all sites except for PRIN. A total of four exceedances were observed at the New Mexico stations using BAM PM_{10} monitors. Both stations recorded exceedances on April 14, 2012 and April 26, 2012 due to high winds.

The site CTSW, west of the cattle facility, recorded two exceedances, with one on April 15 (159 µg/m^3) and another on April 21, 2012 (199 µg/m^3). The CTSO site south of the cattle facility recorded only one exceedance on April 21, 2012 (169 µg/m^3). The FORD station, located on the

far western part of Palomas, exceeded the standard once on April 5, 2012 with a 24-hour PM_{10} concentration of 531 $\mu g/m^3$. On that day, this station recorded the highest PM_{10} throughout the network. In fact one site, CTSW, recoded its lowest value on that day. Exceedances were recorded on April 1 (163 $\mu g/m^3$), April 11 (218 $\mu g/m^3$), and April 23 (305 $\mu g/m^3$). It was interesting to see that none of the Palomas samplers recorded high PM_{10} on those days.

Figure 5.4.1-2 shows all valid MiniVol PM_{10} concentrations during the study. The graph clearly shows PM_{10} concentrations high in the latter part of the study from April 14th to the 23rd. We have found that there is no clear correlation between maximum wind speeds and maximum daily PM_{10} (R^2=0.002). However there is a correlation between daily averaged PM_{10} over the network and daily averaged wind speed (R^2=0.69) for winds over 5 mph (2.2 m/s).

Highest PM_{10} across all sites occurred on April 21, 2012 with a mean PM_{10} concentration of 199 $\mu g/m^3$. Two of the Palomas stations recorded PM_{10} concentrations in excess of the US EPA 24-hour National Ambient Air Quality Standard. 24-hour concentrations varied from 199 $\mu g/m^3$ at CTSW to 65 $\mu g/m^3$ at the FORD site. Winds were not a large factor as the daily mean wind speed was 0.8 m/s with a highest 5-minute maximum wind speed of 6.7 m/s occurring at 5 pm. The daily averaged PM_{10} at the Luna County cattle yard measured 97 $\mu g/m^3$ based on the BAM sampler.

On April 15, the CTSW station recorded the third exceedance of the US EPA 24-hour National Ambient Air Quality Standard. The PM_{10} concentration at CTSW was 159 $\mu g/m^3$ similar to the 146 $\mu g/m^3$ measured at the FORD site. Average PM_{10} across all Palomas sites was 85 $\mu g/m^3$ on this day. Winds may have played a role in these PM_{10} concentrations since the maximum 5-minute wind speed was 12.1 m/s at 1:20 pm while the daily average wind speed was 4 m/s.

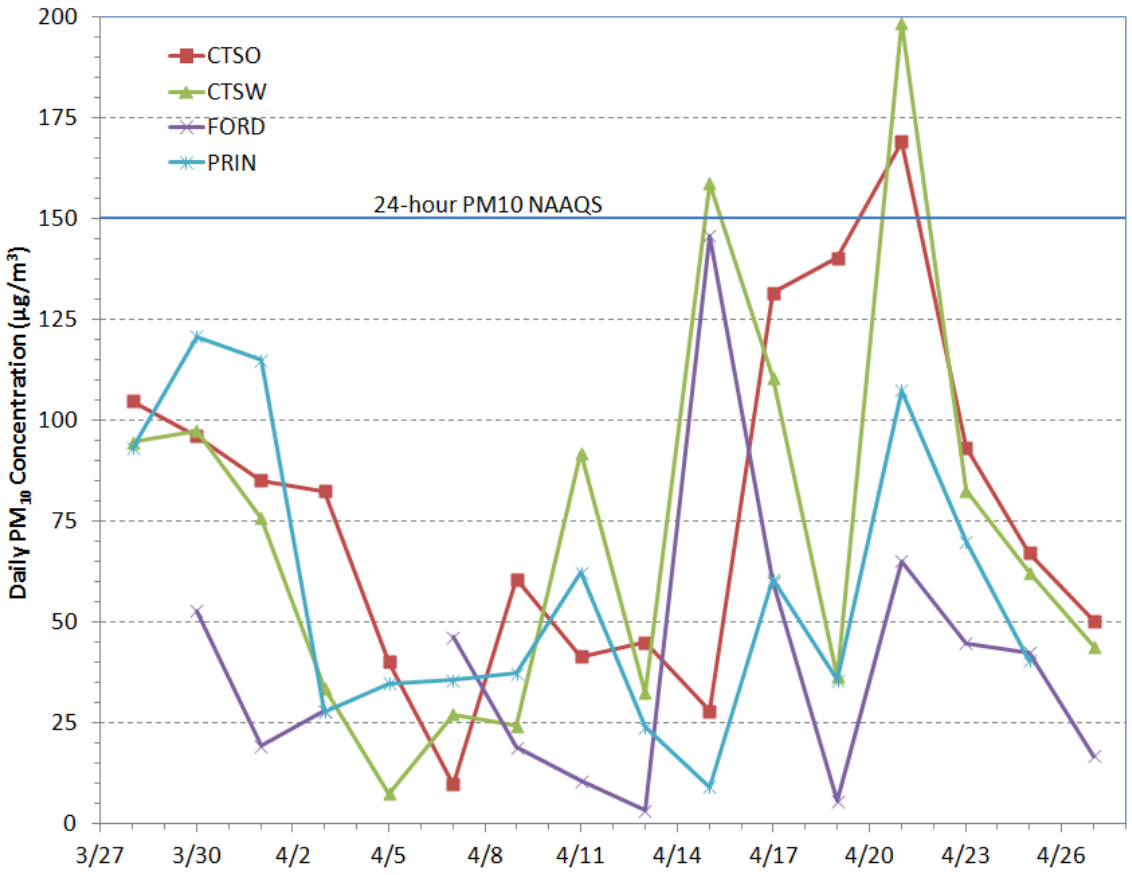

Figure 5.4.1-2. All valid MiniVol 24-hour PM_{10} sample concentrations during the study

5.4.2. Meteorological Conditions

The study occurred during the months of late March and April which are typically highly variable in temperatures and wind with little precipitation. Figure 5.4.2-1 shows the temperatures during study as measured at the CTNE station by the Davis VantagePro weather station. The top line shows the air temperature in degrees Celsius at approximately 3-meters above the ground. The bottom trace is the dew point temperature.

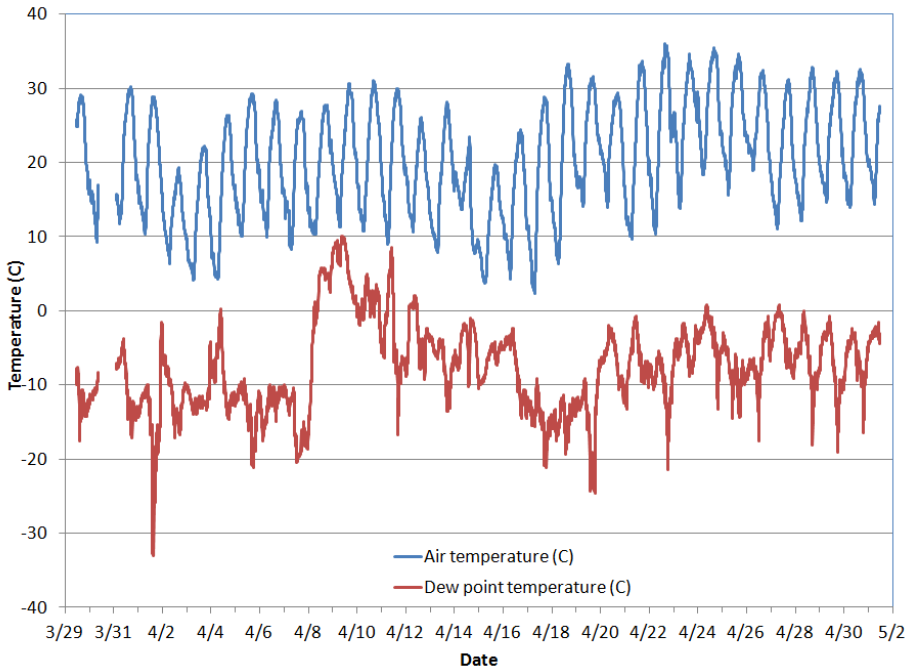

Figure 5.4.2-1. Air temperatures and dew point temperatures through the study measured at the CTSE site

Based on our observations and those at nearby climate stations, it did not rain during the study although relative humidity was high from April 9 to 10 as a storm passed over the area. This is shown in Figure 5.4.2-1 when the difference between the air temperature and dew point temperatures are at their smallest. The majority of the winds were from the westerly directions as show in Figure 5.4.2-2.

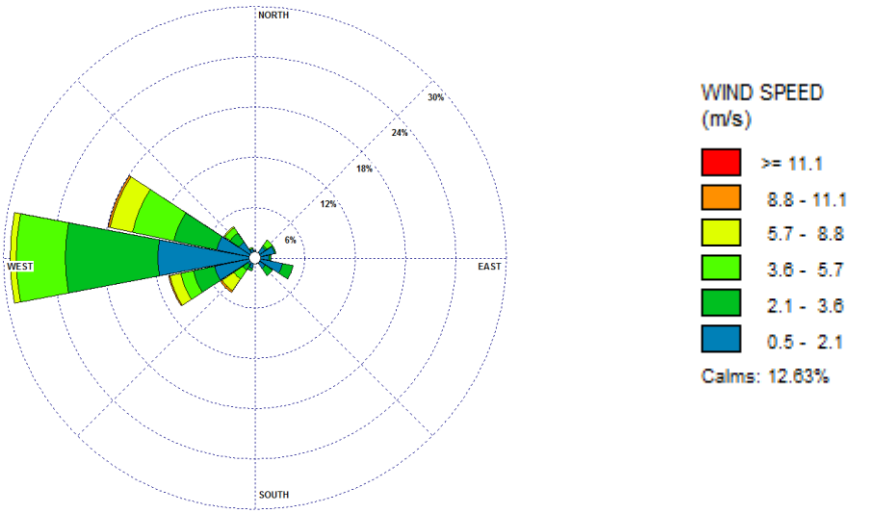

Figure 5.4.2-2. Wind rose showing wind direction statistics during the study at the CTSE site

The highest winds were from the west-northwest, west-southwest, and southwest directions. Figure 5.4.2-3 shows the 5-minute averaged wind speeds and wind gusts during the study. The wind observations were collected at a height of approximately 3-meters above the ground from a Davis Vantage Pro station. Winds shows showed the typical afternoon peaks and low winds during the morning hours.

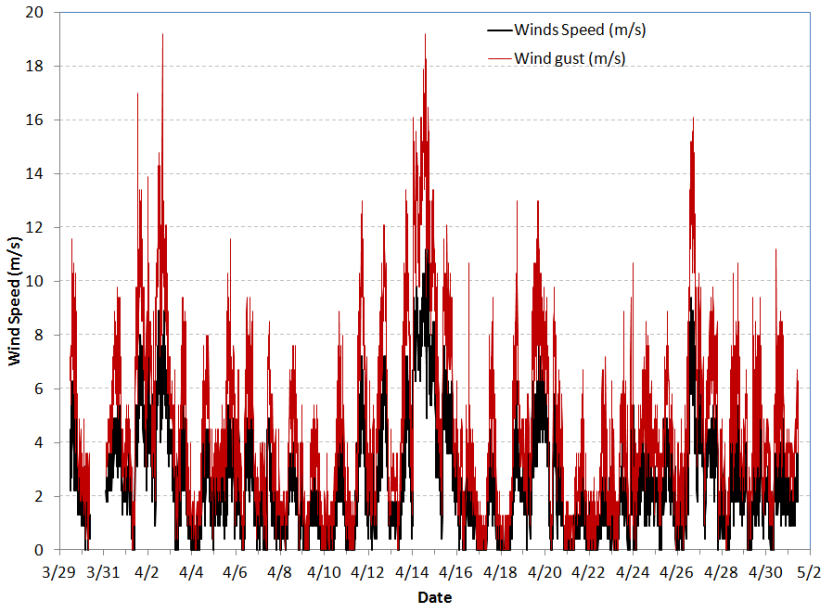

Figure 5.4.2-3. Wind and wind gusts over the duration of the study at the CTSE site

The month of April was both warmer than the long term average and much drier than normal as shown in Figure 5.4.2-4. In fact this climate division experienced the record driest for any April.

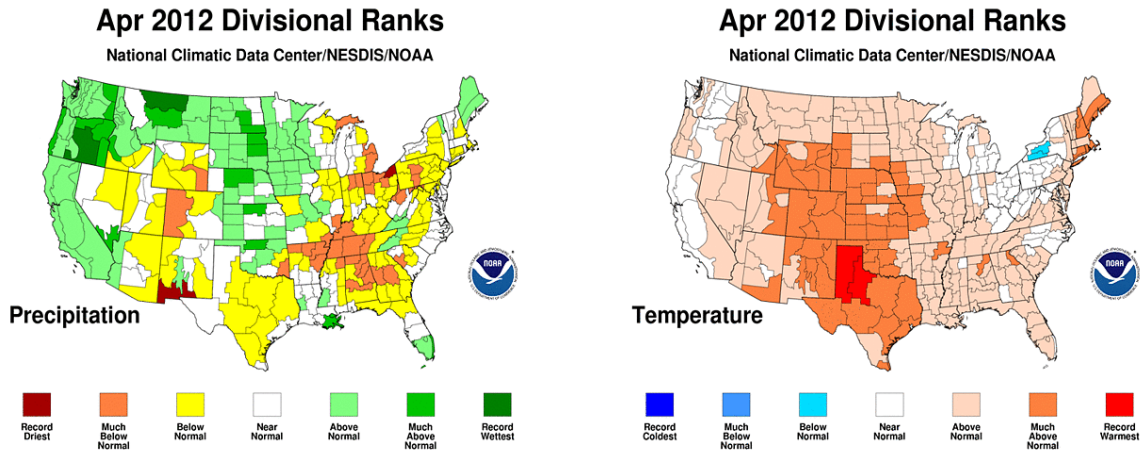

Figure 5.4.2-4. Climate division precipitation (left) and temperature (right) rankings for April 2012.

5.4.3. High Wind Events

An examination of the high wind events are important since they quantitatively indicate when wind erosion occurs and qualitatively show locations where local dust source impacts are

important. The highest PM concentrations are observed at measurement locations closest to the disturbed land, but the deep mixing layers and turbulent updrafts can keep dust particles suspended for transport over long distances. Concentration distributions shift toward the small particle including the $PM_{2.5}$ size fraction with distance from the source as larger particles deposit owing to gravitational settling.

There were three distinct high wind events during the sampling study as shown in Figure 5.4.3-1. The first event occurred on April 2, 2012 but did not produce significant wind erosion. Peak wind measured at the Davis weather station was 43 mph at 3:45 pm. The last it rained in the region was two weeks prior on March 20. The second and most intense in terms of wind speed and PM_{10} concentration occurred on April 14, 2012. The third event occurred on April 26, 2012 and ranked second in terms of peak PM_{10} concentration. Unfortunately both high wind episodes did not coincide with the MiniVol filter sample days but they were captured with the hourly BAM instruments in Columbus.

Figure 5.4.3-1 shows the time series of hourly PM_{10} at both Columbus, New Mexico locations. These two were 735 meters (0.46 mile) apart surrounded in the immediate area by different landuse. The Luna County Cattle monitor was surrounded by cattle pens and a large unpaved lot whereas the Port of Entry station was surrounded partly by a paved lot on the west and open desert to the east. As the plot shows there were two noticeable peaks in aerosol concentrations during the study with both attributed to wind erosion from high winds. The first high wind event occurred on April 14, 2012 with peak hourly PM_{10} of 1920 $\mu g/m^3$ at the Luna cattle facility. On that day there were seven hours where the PM_{10} concentrations were at or near 1000 $\mu g/m^3$.

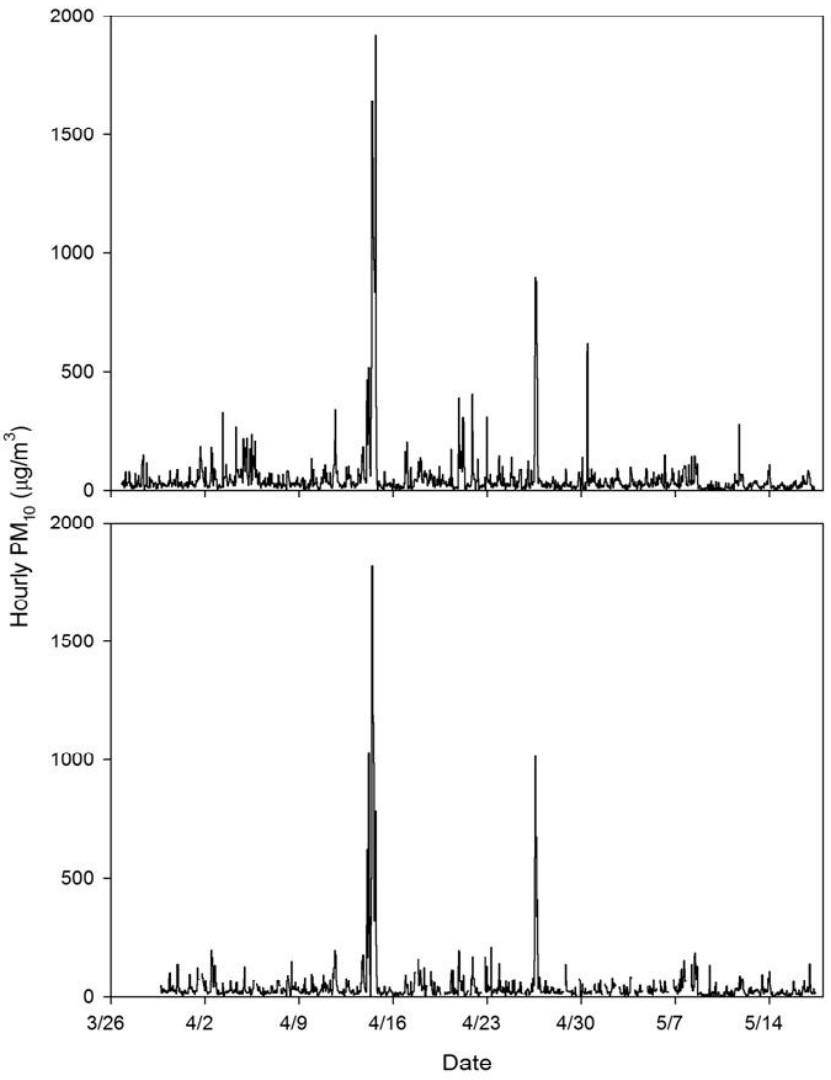

Figure 5.4.3-1. Hourly PM_{10} measured at the Luna County cattle facility (top) compared with Columbus Port of Entry (bottom) using Beta Attenuation Monitors.

It should be noted that the peak concentration the two strongest dust days were similar at both sites. This indicates that during the worst dust events, the dust plume concentrations are similar over this scale. In general there was more variability in daily peak concentrations at the Luna County Cattle facility compared to the Port of Entry and was to be expected give the numerous fugitive dust sources surrounding each monitor.

5.4.3.1. April 14 High Wind Event

This event was triggered by a cold front moving eastward across the state and was responsible for the highest winds and highest PM_{10} concentrations. This storm system brought snow showers to the higher elevations in the Gila Mountains but dry winds to the lower desert of Southwest New Mexico. Winds started early and were observed over 6 m/s (13.4 mph) over most of the day in Columbus. Peak winds on the April 14 as measured by the BAM instrument were 9.9 m/s (22.1 mph) at 5 pm MDT and 43 mph in Palomas at 1:45 pm. Figure 5.4.3.1-1 shows a forecast of surface winds at 1 pm as the cold front moves over the region, extending across Luna County from the SW to NE corners. Winds were from the northwest behind the front and from the west-southwest ahead of the front. On the right of Figure 5.4.3.1-1 is a visible band image from the GOES satellite at 4:02 pm. This image shows an extensive dust plume originating from northern Chihuahua and clearly flowing into the panhandle of Oklahoma.

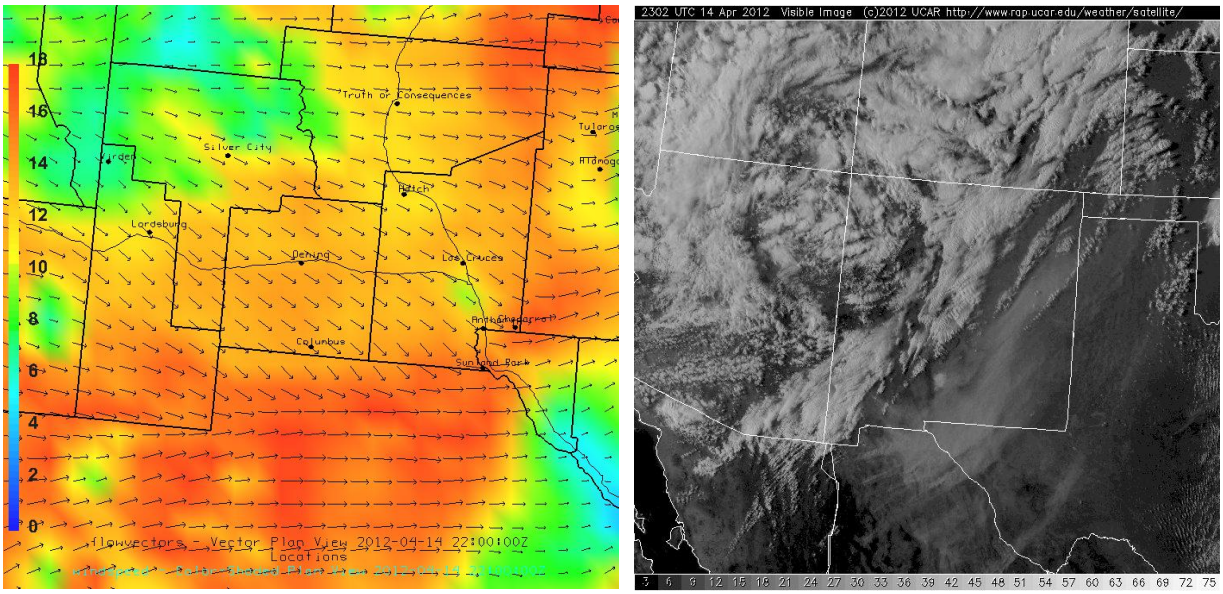

Figure 5.4.3.1-1. Predicted surface winds from the RUC model at 22 UTC (3 pm MDT) on left and GOES visible image at 23:02 UTC (4:02 pm MDT).

Processing the longwave infrared bands of the NOAA AVHRR satellite during this storm revealed that Palomas was on the western edge of the dust plume. Figure 5.4.3.1-2 shows the outline of the plume in relation to the study area.

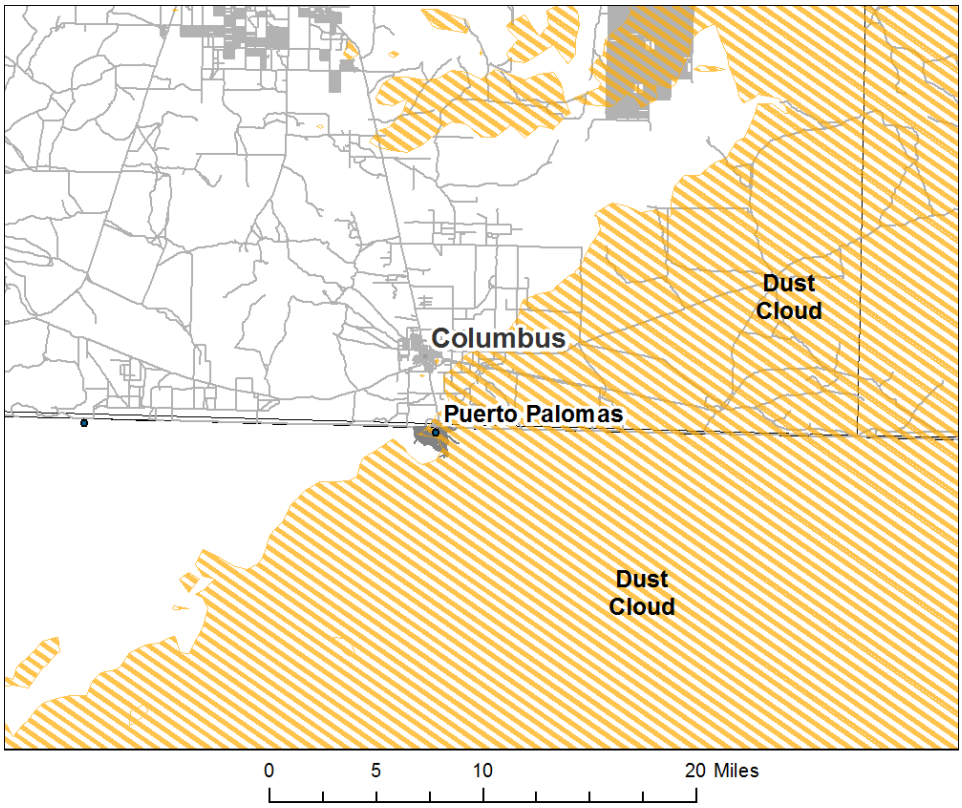

Figure 5.4.3.1-2. Dust plume outline over the Palomas and Columbus region on April 14, 2012

The MiniVol PM_{10} network did not collect data on this day due to the every other day sampling schedule. Both BAMs recorded similar concentrations throughout this dust event as Figure 5.4.3.1-3 shows. The concentrations measured at the Port of Entry sampler however dropped at 3 pm whereas they continued to be high (>900 µg/m^3) for several more hours. In fact the peak PM_{10} occurred at 5 pm at the Luna County cattle facility site.

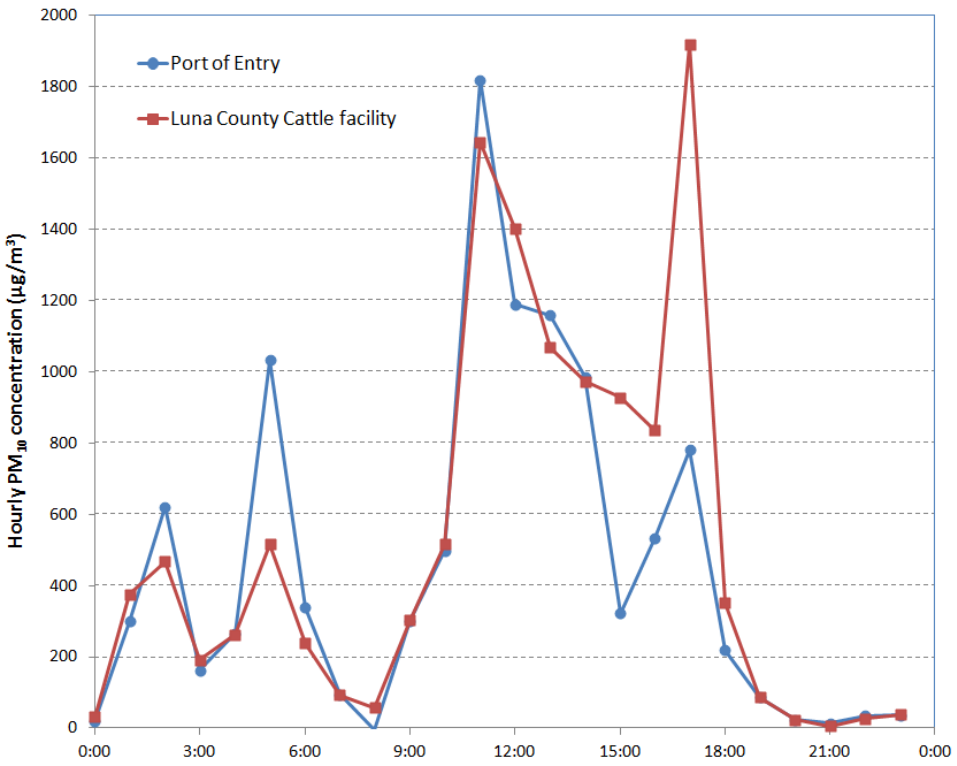

Figure 5.4.3.1-3. Hourly PM_{10} during the April 14, 2012 dust event based on the MetOne BAM. Time on x-axis is local in MDT.

Overall the 24-hour averaged PM_{10} concentration at the Luna County cattle facility was higher at 515 µg/m^3 compared to the Port of Entry value of 451 µg/m^3.

5.4.3.2. April 26 High Wind Event

A quickly moving upper level low and cold front brought in high winds to the border area in the afternoon. The day started off with fairly calm winds in the 2 to 3 m/s range. The forecast for the area predicted winds speeds of 30 to 40 mph with isolated gusts of 50+ mph on east slopes. The National Weather Service also forecasted blowing dust to reduced visibilities to less than a mile in dust prone areas. Peak winds on the April 14 as measured by the BAM instrument were 9.9 m/s (22.1 mph) at 5 pm MDT and 36 mph at 4:50 pm in Palomas. Hourly averaged winds were observed between 6 m/s (13.4 mph) and 7 m/s (15.7 mph) from 3 to 7 pm afternoon in Columbus at the NM DOH satellite station.

Figure 5.4.3.2-1 shows map of the forecasted winds and wind directions from the North American Model (NAM) model for 5 pm on that day. The model predicted the typical southwest wind during from these storms. Strongest winds of the region appear to be over the

Columbus/Palomas area based on the model. On the right side of Figure 5.4.3.2-1 shows a visible GOES satellite image from 5:45 pm and the resulting dust plumes (light gray swaths) from the high winds. Earlier in the day clouds obscured the dust although dust was observed at the ground. Unfortunately clouds obscured on both passes of the MODIS imager on this day.

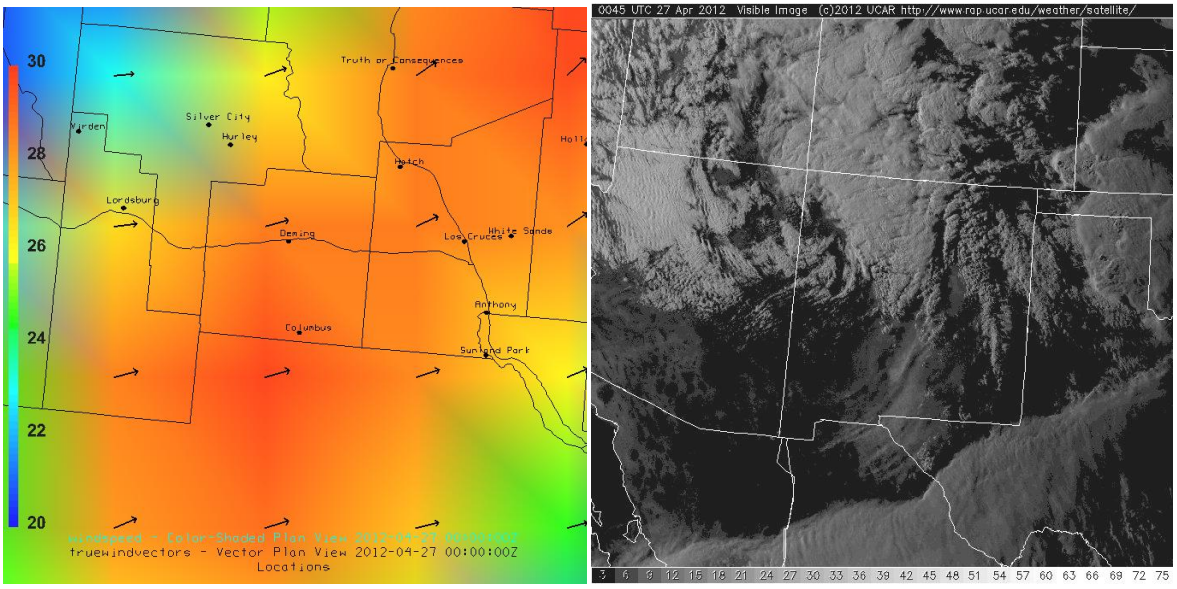

Figure 5.4.3.2-1. Predicted surface winds from the NAM model at 00:00 UTC (5 pm MDT) on left and GOES visible image at 00:45 UTC (5:45 pm MDT).

Similar to the first major dust episode on April 14, the MiniVol PM_{10} network did not collect data on this day due to the every other day sampling schedule. Figure 5.4.3.2-2 shows a time series graph of hourly PM_{10} from the two E-BAMS in Columbus. Note how the two stations recorded similar concentrations with peak PM_{10} on the same hour. This potentially shows that the impacts of the nearby dust sources are equally important at both locations and one is not much more impacted more than the other. Since winds were from the southwest during this episode sources likely responsible include those in the town of Palomas as well as those upwind in the disturbed range lands of Chihuahua.

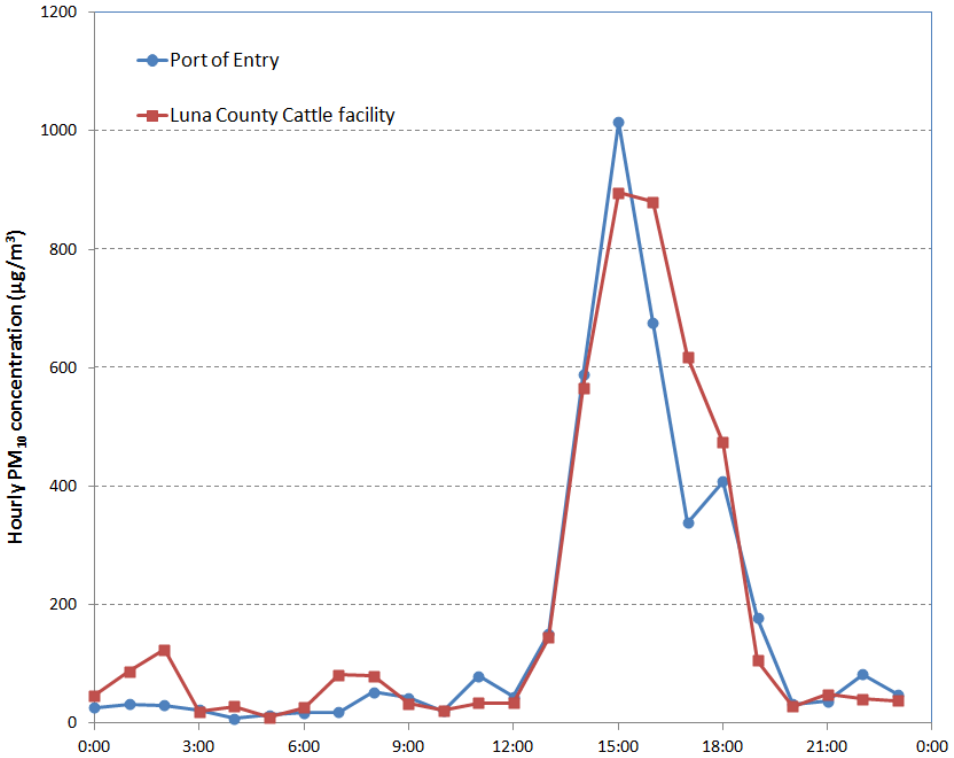

Figure 5.4.3.2-2. Hourly averaged PM_{10} concentrations during the April 26, 2012 high wind dust episode as measured by the MetOne E-BAMs. Time on x-axis is local MDT.

Processing the longwave infrared sounder bands 6 and 8 of the NOAA GOES satellite during this storm revealed that Palomas was on the edge of the dust plume on 23 UTC (5 pm), but likely outside after 00 UTC (6 pm) and 01 UTC (7 pm local). Figure 5.4.3.2-3 shows the outline of the large scale plumes in relation to the study area. The late afternoon satellite passes used in our analysis did not coincide with the highest concentrations measured at the study sites but nevertheless were within the end of the dust episode. Earlier in the day clouds obscured the ground and prohibited a good view of the dust near the peak at around 3 pm MDT.

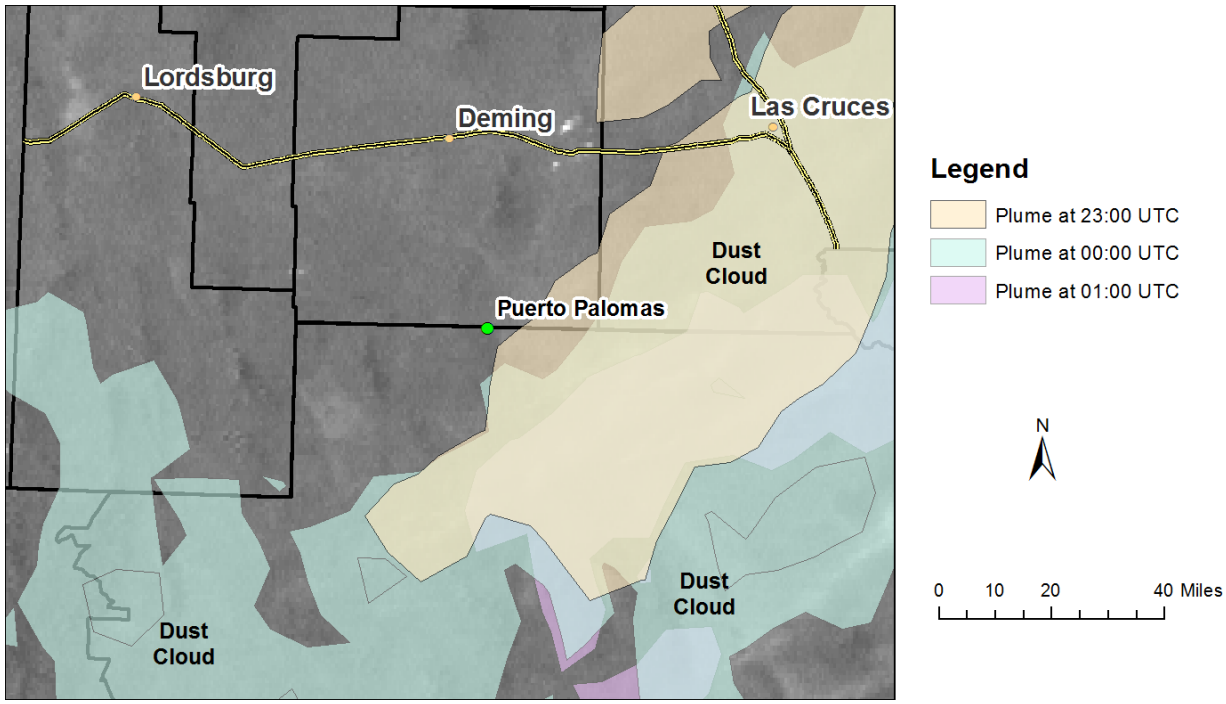

Figure 5.4.3.2-3. Dust plume outlines from April 26, 2012 based on long wave sounder infrared channel satellite imagery at 23, 00, and 01 UTC

5.4.4. Diurnal Patterns

The variation of hourly PM_{10} concentrations can reveal characteristics of the source types and meteorological patterns at a monitoring station. Figure 5.4.4-1 compares the Port of Entry with the Luna County cattle yard hourly PM_{10} data over the whole study. Highest concentrations typically occur in the late afternoon peaking at 4 pm at the Port of Entry while the peak is not a obvious at the cattle yard station although the highest concentrations do occur by 5 pm. In general higher median PM_{10} concentrations also occur during the early morning and late night. Meteorology likely drives this phenomenon since winds are typically lower during those times and prevents pollutant dilution and causes pollutants to remain in the local where they were emitted. For example, a car driving on an unpaved road causes dust generation close to the road and with no wind to disperse it, it will remain in the general area for some time. An interesting feature of both sites is a minimum concentration point in the morning approximately between 8 and 10 am for the 5^{th} through 20^{th} percentile values. The role of meteorology could also play in the role of this since intense mixing of the lower boundary layer starts to intensity as the ground heats up and creates an unstable layer.

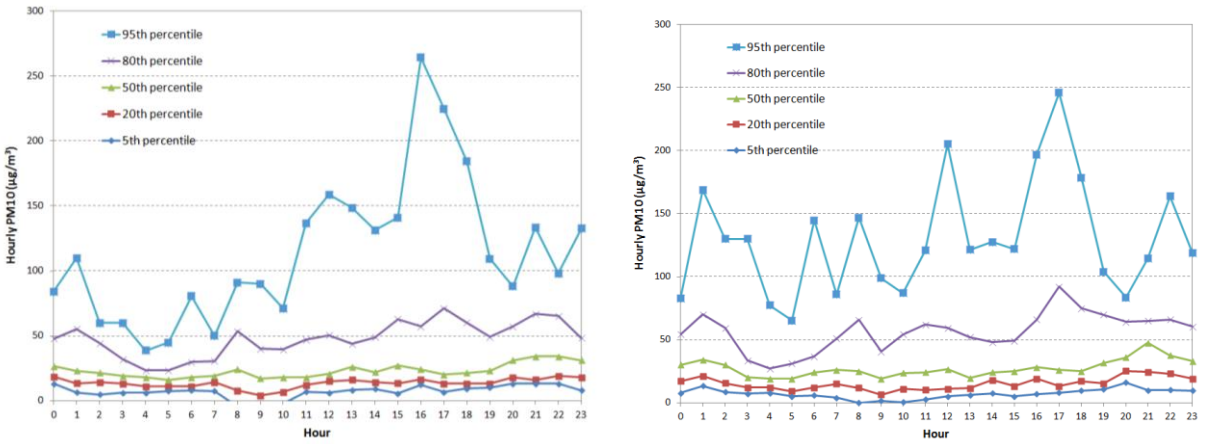

Figure 5.4.4-1. Daily variations in PM_{10} at the Columbus Port of Entry station (left) and Luna County cattle yard (right) by percentile. Each curve represents the specific percentile of that hour of day over the entire study.

An examination of the particle size instrument data provided a view of both the diurnal patterns of particles in Palomas as well as influences from type of emission sources. Figure 5.4.4-2 shows the $PM_{2.5}/PM_{10}$ ratio from April 13 to 16th.

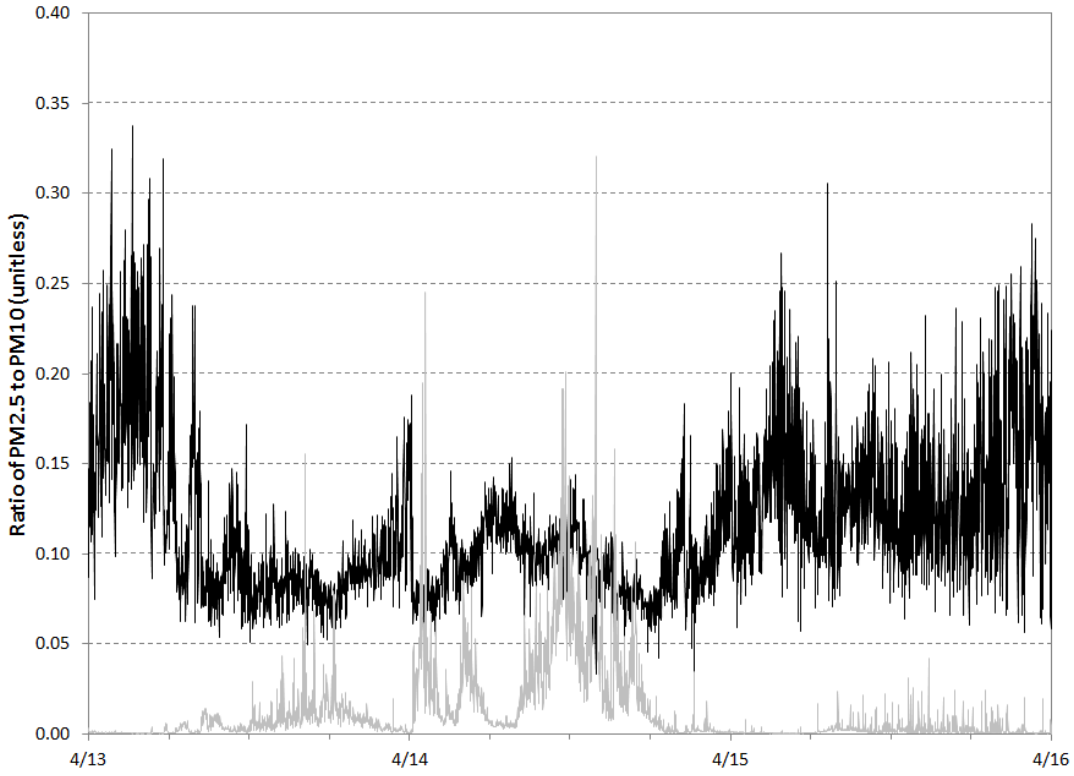

Figure 5.4.4-2. $PM_{2.5}$ to PM_{10} ratio during the April 14, 2012 dust storm. Black trace shows the ratio while the gray line is the PM_{10} data shown on a unitless scale.

Normally during dust storms the ratio is in the 0.10 to 0.12 range based on examination of data from the NMED data. Small ratios indicate particles concentrations are weighted more toward the larger particles and larger rations indicate particles weighted toward smaller particles. Dust storms are dominated by the larger particle sizes since the physical mechanism that produces the dust are typically more than 2 to 3 µm in diameter and most likely larger than 10 µm. When the ratio is high in the 0.4 to 0.8 range, it shows that the particles are dominated by small sizes less than 10 µm and likely less than 1 µm in diameter. Sources for this size of particle include combustion of fuels such as biomass burning or internal combustion engines. Although less likely in this area of the country, they can also be formed in the atmosphere from photochemical and/or thermal reactions.

A day that was influenced by smaller particles occurred on March 30, 2012 after a cold front cooled the area down 20°F compared to the previous day. The ratios greater than 0.3 between 3:00 to 6:00 am show an enhancement of smaller particles that could be from vehicle exhaust, cooking or residential heating. A temperature inversion probably and low winds likely provided the ideal conditions for pollutant such to be observed as these since the low temperature that morning was 49°F. As the sun rose, mixing of the atmosphere dispersed these pollutants and as a result the particle mix was again dominated by larger dust particles. This is evident by the low ratio after 6 am.

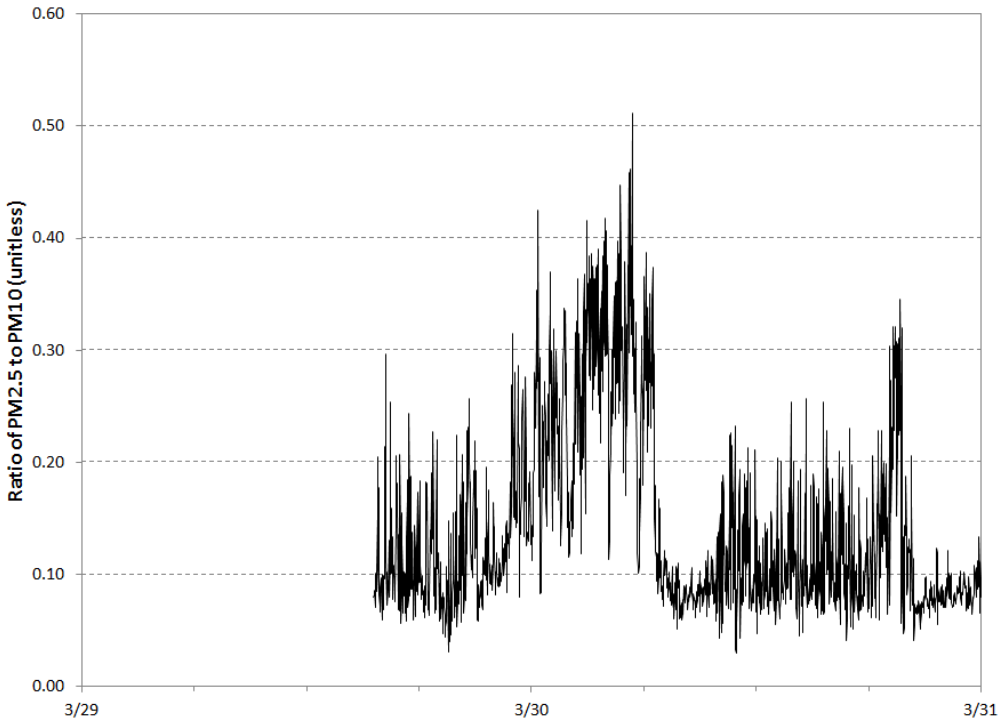

Figure 5.4.4-3. The morning of March 30, 2012 influenced by smaller particles

5.5. Palomas-Columbus Summary

During the study, three exceedances of the 24-hour PM_{10} National Ambient Air Quality Standards were observed in Palomas and two in New Mexico. The two exceedances in New Mexico were during strong dust storms due to high winds. These episodes were not only affected the Palomas/Columbus area but most of southern New Mexico and parts of southern Great Plains as the dust plumes were transported by strong southwesterly winds.

Several conclusions can be drawn from the PM_{10} samples in this study with respect to particle measurements, emission sources, and human exposure. The highest exposures to PM_{10} were from regional dust storms that brought in both transported dust on top of wind blown dust locally generated from erodible areas.

Overall the highest 24-hour averaged PM_{10} concentrations were measured at the CTSO site, south of the cattle facility. PM_{10} concentrations at that site over the study period averaged 78 $\mu g/m^3$ with a median value of 75 $\mu g/m^3$. The second highest average PM_{10} concentrations were measured at the CTSW site, west of the cattle facility. There the average daily PM_{10} was 74 $\mu g/m^3$ and the median value was 69 $\mu g/m^3$.

An analysis of homogeneity across the study PM_{10} network showed that concentrations are highly variable on most days. There were three days when the PM_{10} concentrations varied by more than a factor of 10, and one day when the highest and lowest spanned more than 150 $\mu g/m^3$.

6. Microscopic Analysis of Aerosol Particles

It is informative to examine particle shape (morphology) and quantitative elemental analysis of individual to better understand the samples collected on filters. Particle morphology helps determine the type of source that generated the particle while the elemental analysis provides supporting evidence that type of source.

6.1. Sunland Park PM_{10} and $PM_{2.5}$ Samples

To obtain information on the particle morphologies and quantitative elemental analysis of individual particles we used a scanning electron microscope S-3400N Type II with Noran System Six 300 Nanotrace x-ray microanalysis system. This was done at the NMSU Microscopy Suite of the Core University Research Resources Laboratory (CURRL). A microscopic analysis of the 47 mm PTFE Teflon filters of PM_{10} and $PM_{2.5}$ aerosol collected at the Sunland Park City Yard site to observed individual particle morphologies.

This year we have analyzed filters collected in the spring and early summer of 2012. Most of the particles observed with the energy dispersive x-ray system fit the pattern of particles derived from the soil. In general suspended dust consists mainly of oxides of aluminum, silicon, calcium, titanium, iron, and other metal oxides. In areas surrounded by substantial terrain, eons of runoff produce mineral compositions in soils that can be fairly homogeneous, with the exception of places where dry lake beds exist that have accumulated salt deposits. Industrial processes such as steel making, smelting, and mining have distinct geological compositions. For instance, cement production and distribution facilities may use alcareous, siliceous, argillaceous and ferriferous minerals that may not be natural to the region, with limestone ($CaCO_3$) being the most abundant (Greer et al., 1992). Suspended geological material resides mostly in the coarse particle fraction (Houck et al., 1989, 1990) and typically constitutes ~50% of PM_{10}, while only contributing 5 to 15% of $PM_{2.5}$ (Watson et al., 1994).

Figure 6.1-1 shows an example of a micron-sized particle's elemental composition and morphology from a sample collected at the Sunland Park City Yard site. Particles show up as the lighter gray and white. The background substrate material from the PTFE filter shows up as the darkest shades and black. The x-ray spectrum at the point shown with a cross-hair is shown on the right side of the figure. As the spectrum shows there are strong counts of calcium, silicon, and iron that are indicative of a particle with a geological origin. The particle in question had a physical dimension of approximately 1 µm in diameter. In the x-ray spectrum the PTFE substrate gives a strong peak at 0.7 KeV corresponding to fluorine.

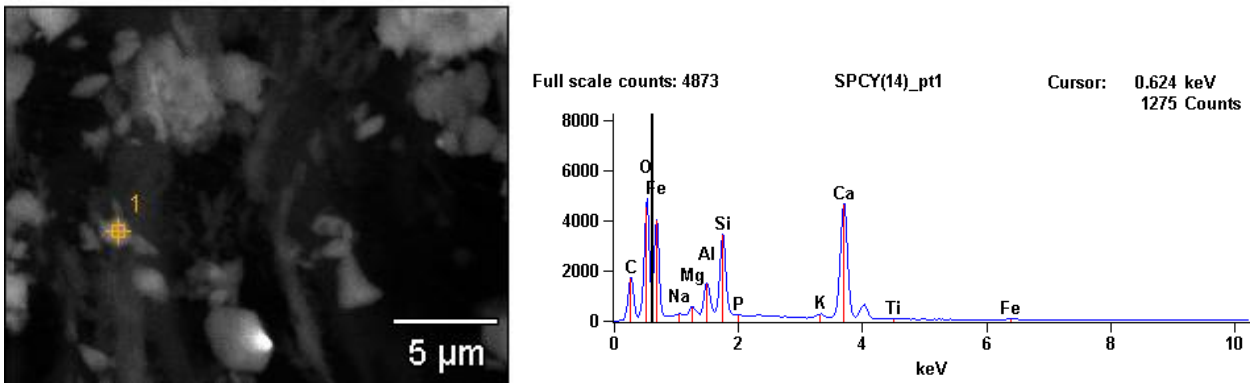

Figure 6.1-1. Example of particle x-ray spectrum of Sunland Park sample. Magnification was 5500x.

Another sample with a large particle with approximate 25 µm physical diameter is shown in Figure 6.1-2. The elemental spectrum is different than the example above with a lesser amount of calcium and a stronger titanium signal. This particle is also classified as a soil particle. As the figure shows, there are many smaller particles embedded on the PTFE filter a few large particles that penetrated through the PM_{10} impactor plate.

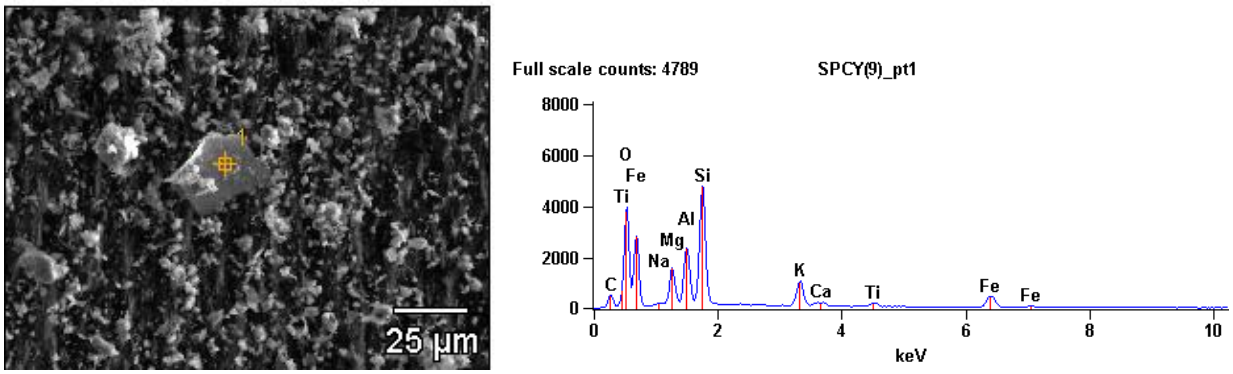

Figure 6.1-2 Example of large 25 µm soil particle x-ray spectrum of Sunland Park sample. Magnification was 800x.

Searching for particles other than soil proved to be difficult in the 24-hour Sunland Park samples. Relatively spherical particles such as that in Figure 6.1-3 often look like combustion or soot but in fact they appear to be soil after probing them with the x-ray spectrometer.

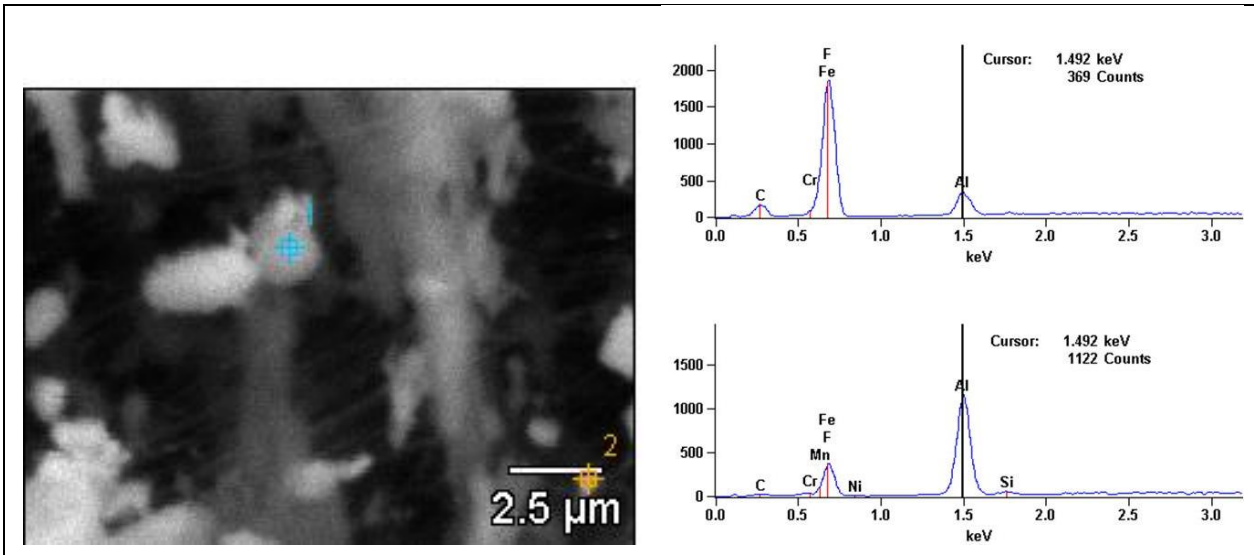

Figure 6.1-3. Small spherical particle from Sunland Park site

Analysis of more filters including those from the low wind high PM events will be analyzed in FY2013 and compared to those collected in the spring and summer.

6.2. Wind Erosion Samples

Samples collected on rotoslide samplers were viewed under the scanning electron microscope to obtain particle sizes and morphologies. We used Hitachi S-3400N Type II SEM. Rotoslide samplers where attached to a pole at 2, 4, and 6 feet above the ground. We took samples at seven locations this year. Table 6.2-1 provides the locations and dates of sampling.

Table 6.2-1. Locations and dates of dust particle sampling from unpaved roads and wind erosion

Location	Dates of samples
Leyendecker farm, south of Las Cruces	2/17/2011, 8/23/2011
Roadrunner Parkway, east side of Las Cruces	2/17/2011, 9/1/2011
Columbus	8/25/2011
Deming	8/25/2011
Anthony	8/27/2011
Mexico playa	
Cd. Juarez	3/7/2011,3/21/2011, 4/3/2011, 4/9/2011, 4/26/2011 and 4/29/2011

The technique used to measure air dispersed particulate matter (PM) was a small tower formed by a steel tube of 2.5 cm diameter and 2.5 m high, which was placed 1 m and a rotor another to 2 m. Each of the rotors had two wings each wing and a piece of tape 2 x 5.5 cm attached to a transparent glass slide of 2.5 x 7.5 cm (Figure 6.2-1) for trapping particulate.

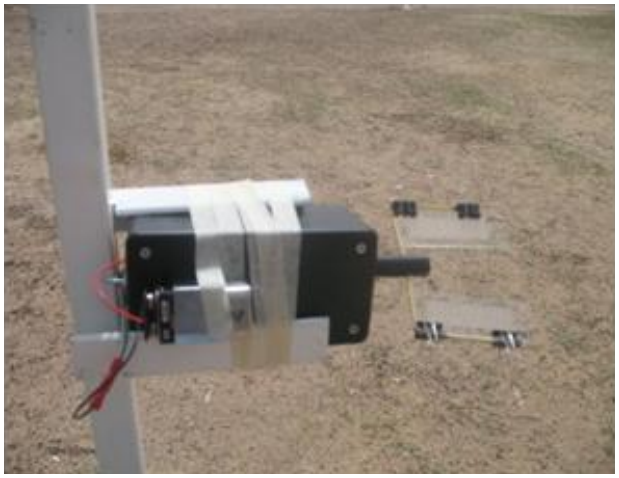

Figure 6.2-1. Rotoslide sampler as attached to sampling pole.

The weight of the slide with the tape was recorded prior to sampling, this will use a digital scale and used four digits for better data accuracy. The cover tape is removed when initiating the measurement was also heavy to be used in the calculation of PM adhered to the tape. PM measurements consisted in having the rotors turned on for periods of 30 minutes and changing the tapes, in each case the PM tapes were placed in plastic slide boxes to prevent tampering and subsequent weight record in the laboratory. The speed of each rotor was recorded at the beginning and end of each of the measurements. The total volume of air sampled is determined

from the revolutions per minute (rpm) known of the rotors, the circumference of the area sampled (π * transverse diameter circle during one rotation or π * d) and based on the dimensions Adhesive tape (length L and width, w) using the following relationship:

Total volume sampled per minute = π * d * L * W * rpm * 2

In this equation, the doubling was done because it had two tapes in each set of rotor (Flores et al., 2011). Weather conditions, especially wind direction and speed were recorded by monitoring stations of the Autonomous University of Ciudad Juarez. Data analysis consisted of descriptive statistics as mean, standard deviation and range, comparison of averages between sampling sites using the statistical package SPSS version 17.0.

The strongest wind conditions recorded in this study are shown in Figure 6.2-2, where higher wind gusts were 66 to 70 km/hr in March and April, while the maximum observed speeds were 48 and 53 km/hr.

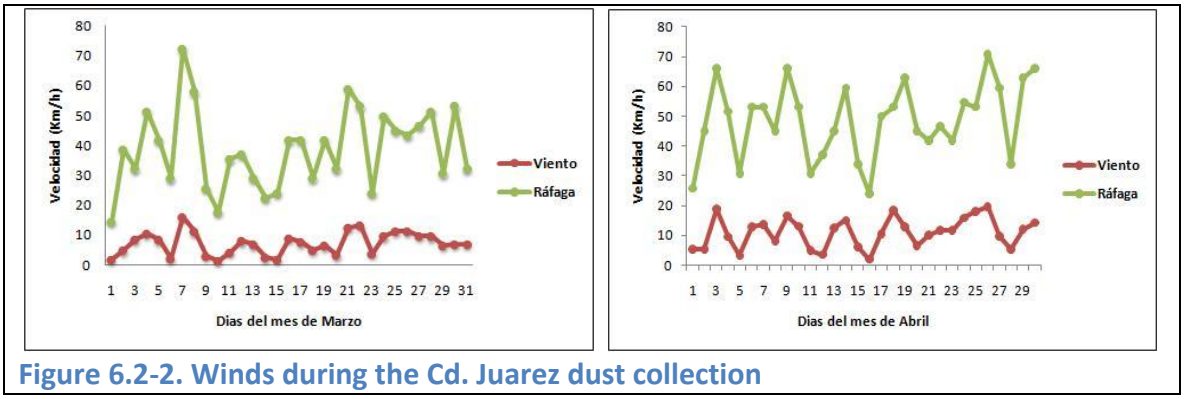

Figure 6.2-2. Winds during the Cd. Juarez dust collection

During these weather events were conducted PM estimates at four sites in the city, for this is shown in Figure 6.2-3. PM concentrations detected at 1 and 2 m above ground level. The concentration of PM adhering to the tape on slides for periods of 30 minutes in the four sampling sites presented a range of 0 to 2.7667 ± 1.0356 mg/m^3 and an average of 0.65074 ± 0.0894 mg/m^3. These data indicate a natural emission of PM from 0 to 2.7667 mg/m^3, which is greater than the Environmental Standards and shows poor air quality during these events that have a potential effect on the health of people and a high risk of accidents due to low visibility (NOM-025-SSA1-1993). This regulation outlines the value in the acute exposure limit of 150 µg/m^3 in 24 hours and chronic exposure of 50 µg/m^3 annual average for health protection of the susceptible population. Meanwhile, the Environmental Protection Agency of the United States (U.S. EPA) in 2006 changed 24-hour $PM_{2.5}$ standard from 65 to 35 ug/m^3. The average of the four sites studied, the amount of PM retained on the tape was greater at 1-m above the ground, 0.698852 ± 0.08537 mg/m^3 than 2-m high, ± 0.093615 0.599964 mg/m^3, but not significantly difference, which is explained by the greater weight of large particles that are

transported to lower altitudes and may be retained by adhesive tapes. Sites 1 and 4 had greater clarity in capturing PM at 1 m, while sites 1 and 3 had the 2-m concentration higher (Figure 6.2-3). As the occurrence of winds and its intensity was highly variable, it was simple to detect differences between sampling dates and locations, but the month of April was the one that showed higher winds.

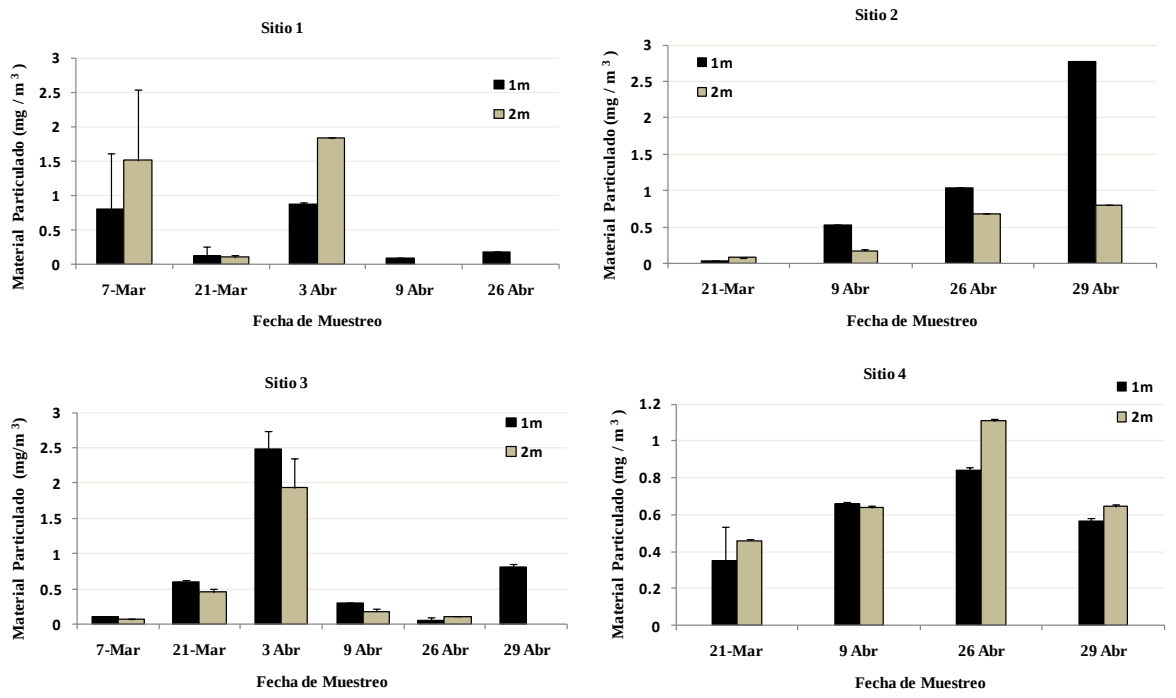

Figure 6.2-3. Comparison of samples collected in Cd. Juarez at two heights 1 and 2 meters above the ground.

The amount of PM trapped by the sticky tape samples in the four sampling sites ranged from 0 to 2.7667 ± 1.0356 mg/m^3 with an average of 0.65074 ± 0.0894 mg/m^3. These data were higher than the values reported by the Official Statement and reflected poor air quality during the study and the potential negative effects on the population's respiratory health. The technique based on rotorod and tapes was considered practical, economical and versatile for measuring particulates in dust storms, which in future studies could be validated by correlations with automated instruments for measuring particles under different climate scenarios and soil types.

7. References

Anderson HR, Atkinson RW, Peacock JL, Marston L, Konstantinou K. (2004) Meta-analysis of time-series studies and panel studies of particulate matter (PM) and ozone. Report of a WHO

task group. World Health Organization. http://www.euro.who.int/document/e82792.pdf Last accessed on January 2012

California Air Resources Board (2005) Review of the California Ambient Air Quality Standard for Ozone http://www.arb.ca.gov/research/aaqs/ozone-rs/ch10.pdf Lasr accessed on February 2012

Causes of Haze Assessment (2006) http://coha.dri.edu/web/general/trajgallery/trajmapgallery.html Last accessed on January 20, 2012.

Flannigan MD, Logan KA, Amiro BD, Skinner WR, Stocks BJ (2004) Future area burned in Canada. Clim Change 72:1-16.

Flores, M.J.P., M. Shukla y B. Hernández. 2011. Material particulado dispersado al aire por vehículos en caminos agrícolas no pavimentados. Terra Latinoamericana, 29(1):23-34.

Gillet NP, Weaver AJ, Zwiers FW, Flannigan MD (2004) Detecting the effect of climate change on Canadian forest fires Geophys Res Lett doi:101029/2004GL020876.

Greer,W.L.; Johnson,M.D.; Morton,E.L.; Raught,E.C.; Steuch,H.E.; and Trusty,C.B. (1992). Portland cement. In Air Pollution Engineering Manual, Buonicore,A.J. and Davis,W.T., Eds. Van Nostrand Reinhold, New York, NY, pp. 746-766.

Houck,J.E.; Chow,J.C.; and Ahuja,M.S. (1989). The chemical and size characterization of particulate material originating from geological sources in California. In Transactions, Receptor Models in Air Resources Management, Watson,J.G., Ed. Air & Waste Management Association, Pittsburgh, PA, pp. 322-333.

Houck,J.E.; Chow,J.C.; Watson,J.G.; Simons,C.A.; Pritchett,L.C.; Goulet,J.M.; and Frazier,C.A. (1989). Determination of particle size distribution and chemical composition of particulate matter from selected sources in California. Prepared for California Air Resources Board, Sacramento, CA, by OMNI Environmental Services, Inc. and Desert Research Institute, Beaverton, OR and Reno, NV.

Houck,J.E.; Goulet,J.M.; Chow,J.C.; Watson,J.G.; and Pritchett,L.C. (1990). Chemical characterization of emission sources contributing to light extinction. In Transactions, Visibility and Fine Particles, Mathai,C.V., Ed. Air and Waste Management Association, Pittsburgh, PA, pp. 437-446.

IMIP (Instituto Municipal de Investigación y Planeación). 2010. Mapa de calles pavimentados y sin pavimentar en Ciudad Juárez, Chihuahua, México. www.imip.org.mx.

Jaffe D, Bertschi I, Jaegle L, Novelli P, Reid JS, Tanimoto H, Vingarzan R, Westphal DL (2004) Long-range transport of Siberian biomass burning emissions and impact on surface ozone in western North America. Geophys Res Lett doi:10.1029/2004GL020093.

Ji M, Cohan DS, Bell ML (2011) Meta-analysis of the association between short-term exposure to ambient ozone and respiratory hospital admissions. Environ. Res. Lett. 6, 1-11

Junquera V, Russell MM, Vizuete W, Kimura Y, Allen D (2005) Wildfires in eastern Texas in August and September 2000: Emissions, aircraft measurements, and impact on photochemistry. Atmos Environ 39:4983-4996.

Lianou M, Chalbot M-C, Kotronarou A, Kavouras IG, Karakatsani A, Katsouyanni K, Puustinnen A, Hameri K, Vallius M, Pekkanen J, Meddings C, Harrison RM, Thomas S, Ayres JG, ten Brink H, Kos G, Meliefste K, de Hartog J, Hoek G (2007) Dependence of outdoor particulate mass and number concentrations on residential and traffic features in urban areas. J Air Waste Manag Assoc 57:1507-1517.

Mar TF, Koenig JQ (2009) Relationship between visits to emergency departments for asthma and ozone exposure in greater Seattle, Washington. Ann Allergy Asthma Immunol 103, 474-479

Norma Oficial Mexicana (NOM-025-SSA1-1993). Criterios Para Evaluar el Valor Límite Permisible Para la Concentración de Material Particulado. Valor Limite Permisible Para la Concentración de Partículas Suspendidas Totales (PST), Partículas Menores de 10 Micrómetros (PM10) y Partículas Menores de 2.5 Micrómetros (PM2.5) de la Calidad del Aire Ambiente. Criterios Para Evaluar la Calidad Del Aire. Secretaria de Salud. México.

Pfister GG, Emmons LK, Hess PG, Honrath R, Lamarque JF, Martin MV, Owen RC, Avery MA, Browell EV, Holloway JS, Nedelec P, Purvis R, Ryerson TB, Sachse GW, Schlager H (2006) Ozone production from the 2004 North American boreal fires. J Geophys Res Atmos doi:10.1029/2006JD007695.

Pinto JP, Lefohn AS, Shadwick DS (2004) Spatial variability of PM2.5 in urban areas in the United States. J Air Wastes manag Assoc 34: 4193-4204.

Rivera Rivera, N.I., Gill, T.E., Bleiweiss, M.P. y Hand, J.L. 2010. Source Characteristics of Hazardous Chihuahuan Desert dust outbreaks. Atmospheric environment, 44:2457-2468.

Romieu I, Aquilar MR, Macias HM, Villareal AB, Cadena LH, Arroyo LC (2003) Health impacts of air pollution on morbidity and mortality among children of Cuidad Juarez, Chihuahua, Mexico, Commision for Environmental Cooperation of North America. http://www.cec.org/Storage/52/4453_cdjuarez_en.pdf Last accessed on February 2012.

Running SW (2006) Is global warming causing more larger wildfires? Science, 313, 927-928.

Schnell RC, Oltmans SJ, Neely RR, Endres MS, Molenar JV, White AB (2009) Rapid photochemical production of ozone at high concentrations in a rural site during winter. Nature Geo 2:120-122.

Schoennagel T, Veblen TT, Romme WH (2004) The interaction of fire, fuels, and climate across Rocky Mountain Forests. BioScience 54:661-676.

Schwartz, J., D. Dockery y L. Neas. 1996. "Is Daily Mortality Associated Specifically With Fine Particles?" Journal of the Air and Waste Management Association. 46: 927-939.

Spracklen DV, Logan JA, Mickey LJ, Park RJ, Yevich R, Westerling AL, Jaffe DA (2007) Wildfires drive interannual variability of organic carbon aerosol on the western US in summer. Geophys Res Lett doi:101029/2007GL030037.

Stocks BJ, Mason JA, Todd JB, Bosch EM, WottonBM, AmiroBD, Flannigan MD, Hirsch KG, Logan KA, Martell DL, Skinner WR (2002) Large forest fires in Canada, 1959-1997. J Geophys Res doi:101029/2001JD000484.

Thurston GD, Ito K (2001) Epidemiological studies of acute ozone exposures and mortality. J Expo Anal Environ Epidemiol 11, 286-294.

Tolbert PE, Mulholland JA, MacIntosh DL, Xu F, Daniels D, Devine OJ, Carlin BP, Klein M, Dorley J, Butler AJ, Nordenberg DF, Frumkin H, Ryan PB, White MC. 2000. Air quality and pediatric emergency room visits for asthma in Atlanta, Georgia, USA. Am J Epidemiol 151, 798-810.

U.S.EPA, 2006. Particulate Matter, PM Standards. Effective December 17, 2006. http://www.epa.gov/air/particlepollution/standards.html>. Disponible Marzo de 2011.

US Environmental Protection Agency, Federal Register, Volume 62, Number 138, ''National Ambient Air Quality Standards for Ozone: Final Rule,'' pages 38855–38896, Washington, D.C., July 18, 1997. Available from: http://www.epa. gov/ttn/naaqs/ozone/ozonetech/a18580.htm Last accessed February 1, 2012.

US Environmental Protection Agency, Federal Register, Volume 73, Number 60, ''National Ambient Air Quality Standards for Ozone: Final Rule,'' pages 16436–16514, Washington, D.C., March 27, 2008. Available from: http://edocket. access.gpo.gov/2008/pdf/e8-5645.pdf Last accessed February 1, 2012.

US EPA, Area Designations for 2008 Ground-level Ozone Standards, January 2011 http://www.epa.gov/ozonedesignations/2008standards/state.htm Last accessed on February 5, 2012

Watson,J.G.; Chow,J.C.; Lu,Z.; Fujita,E.M.; Lowenthal,D.H.; and Lawson,D.R. (1994). Chemical mass balance source apportionment of PM10 during the Southern California Air Quality Study. Aerosol Sci. Technol., 21:1-36.

Westerling AL, Hidalgo HG, Cayan DR, Swetnam TW (2006) Warming and earlier spring increase western US forest wildfire activity. Science 313:940-943.

WHO, 2000. Guidelines for Air Quality. World Health Organization, Geneva. 190 p.

William, D.S, Shukla, M.K, Ross,J. 2008. Particulate matter emission by a vehicle running on unpaved road. Atmospheric Environment, (42): 3899-3905.